SYNTHESIS OF TITANIUM-BASED POWDERS FROM MACHINING WASTE BY USING THE HYDROGENATION-DEHYDROGENATION METHOD

A Thesis Submitted to
the Graduate School of
İzmir Institute of Technology
in Partial Fulfillment of the Requirements for the Degree of
MASTER OF SCIENCE

in Materials Science and Engineering

by

Zeynep ÇUHADAROĞLU

July 2022

İZMİR

ACKNOWLEDGEMENTS

First and foremost, I express my sincere gratitude to my thesis advisor, Dr. Mertol Gökelma, who has been a continuous source of inspiration, encouragement, and intellectual stimulation. I am grateful to him for letting me work on such an exciting topic, through which I could build both my exposition and characterization skills. I appreciate his confidence in me throughout my research work with him. His far-reaching vision, invaluable guidance, and great support made this thesis possible.
I am also very grateful to my co-advisor, Aziz Genç, and jury members Mustafa Güden and Onur Ertuğrul for their insightful comments and motivations.
My appreciation also goes to my colleagues, İrem Yaren Çapkın, Alireza Habibzadeh, Rabia Önen, and, Pınar Yörük in our research group who supported my research activities.

I must express my special thanks to my adorable boyfriend, Bora Doğaroğlu, for his love, scientific support, and unwavering patience during this challenging journey. Without his contribution, this accomplishment would have been vastly more difficult.

I wish to thank all my family and friends Selen Akar, Leyla Akbalık, Dilan Akyüz, Özge Özçelik, İnan Özdemir and Cansu Şen for their support. I dedicate this thesis to my lovely family.

This thesis is supported by the Scientific and Technological Research Council of Turkey (TÜBİTAK-118C311).

ABSTRACT

SYNTHESIS OF TITANIUM-BASED POWDERS FROM MACHINING WASTE BY USING THE HYDROGENATION-DEHYDROGENATION METHOD

Sustainability and recycling activities have gained importance in almost every field all over the world. Many studies are conducted to recycle titanium and titanium alloys owing to their outstanding properties like low density, biocompatibility, corrosion resistance, and high strength-to-weight ratio. Although they offer superior properties, their usage is limited due to their high production cost and potential to generate waste, and therefore, recycling activities in this area should be expanded using an appropriate method. Cold hearth melting, vacuum arc re-melting, and hydrogenation and dehydrogenation process are widely used for recycling titanium scraps in industry. Among them, the hydrogenation and dehydrogenation (HDH) process has a significant environmental and economic impact. In this thesis, titanium powders were synthesized from additive manufacturing turnings. Ti-6Al-2Sn-4Zr-6Mo turnings were used as starting materials on which HDH characteristics were not investigated in the literature. Both hydrogenation and dehydrogenation parameters were studied to reach optimum conditions. Our results revealed that hydrogenation was accomplished at 500 °C for 120 minutes with 5 °C/minute heating rate. The optimum dehydrogenation condition was found at 600 °C for 90 minutes. Ti-6Al-2Sn-4Zr-6Mo powder with average 56 μm particle size was synthesized; however, hydrogen and oxygen concentrations in the powder were not at the desired level and non-spherical shaped powders were produced end of the process.

ÖZET

HİDROJENASYON-DEHİDROJENASYON YÖNTEMİ KULLANILARAK TALAŞLI İMALAT ATIKLARINDAN TİTANYUM BAZLI TOZLARIN SENTEZLENMESİ

Sürdürülebilirlik ve geri dönüşüm faaliyetleri tüm dünyada hemen her alanda önem kazanmıştır. Düşük yoğunluk, biyouyumluluk, korozyon direnci ve yüksek mukavemet/ağırlık oranı gibi üstün özelliklerinden dolayı titanyum ve titanyum alaşımlarının geri dönüşümü için birçok çalışma yapılmaktadır. Üstün özellikler sunmalarına rağmen, yüksek üretim maliyetleri ve atık üretme potansiyelleri nedeniyle titanyum ve alaşımlarının kullanımları sınırlıdır ve bu nedenle bu alandaki geri dönüşüm faaliyetleri uygun bir yöntemle yaygınlaştırılmalıdır. Soğuk ocak eritme, vakum ark yeniden eritme ve hidrojenasyon ve dehidrojenasyon prosesleri, endüstride titanyum atıklarının geri dönüştürülmesi için yaygın olarak kullanılmaktadır. Bunlar arasında hidrojenasyon ve dehidrojenasyon (HDH) prosesinin büyük bir çevresel ve ekonomik etkisi vardır. Bu tezde, eklemeli imalat atıklarından titanyum tozları sentezlendi. Literatürde HDH özellikleri araştırılmayan Ti-6Al-2Sn-4Zr-6Mo atıkları başlangıç malzemesi olarak kullanılmıştır. Optimum koşullara ulaşmak için hem hidrojenasyon hem de dehidrojenasyon parametreleri incelenmiştir. Sonuçlarımız hidrojenasyonun 500 °C'de 120 dakika boyunca 5 °C/dakika ısıtma hızıyla gerçekleştirildiğini ortaya koydu. Optimum dehidrojenasyon koşulu 600 °C'de 90 dakika olarak bulundu. Ortalama 56 μm tanecik boyutuna sahip Ti-6Al-2Sn-4Zr-6Mo tozu sentezlendi; ancak tozdaki hidrojen ve oksijen konsantrasyonları istenilen düzeyde değildi ve işlem sonunda küresel olmayan tozlar üretildi.

Dedicated to my lovely family…

TABLE OF CONTENTS

LIST OF FIGURES

Figure **Page**

Figure **Page**

Figure **Page**

LIST OF TABLES

Table **Page**

LIST OF ABBREVIATIONS

BE Blended elemental

bcc Body-centered cubic structure

CHM Cold hearth melting

CP-Ti Commercially pure titanium

hcp Hexagonal close-packed

HDH Hydrogenation -Dehydrogenation

PA Pre-alloyed

P/M Powder Metallurgy

SEM Scanning Electron Microscopy

TGA Thermogravimetric Analysis

VAR Vacuum arc re-melting

CHAPTER 1

INTRODUCTION

Compared to competing materials, including aluminium and stainless steel, titanium and its alloys offer outstanding properties like low density with high strength, excellent corrosion resistance, and biocompatibility, making them attractive materials in several branches of industry. Nonetheless, their usage is restricted owing to their high cost, despite their superior properties.

Besides their outstanding properties, they have high oxygen affinities, low thermal conductivities, and modulus of elasticity, leading to waste generation during the fabrication and forming process. The increasing consumption of metal resources in the world and the resulting increase in the amount of waste have led to the establishment of recycling technologies in many fields. Many studies have been carried out on recycling titanium and its alloys, considering their high cost and capability of waste generation.

Powder metallurgy is a cost-effective route with little waste generation in which titanium and its alloys have been extensively used. There are several methods to obtain titanium powder, including Atomization, Armstrong, Fray-Farthing-Chen Cambridge, and Hydrogenation-Dehydrogenation. The hydrogenation-dehydrogenation (HDH) process has a significant economic and environmental impact where powder production is based on hydrogen embrittlement, the reaction takes place in a solid-state, and secondary sources can be used as raw material.

From the wide usage in titanium markets and waste generation point of view, most researchers have focused on synthesizing titanium powder from Ti-6Al-4V secondary sources by using the hydrogenation-dehydrogenation method. There have been no reports on the hydrogenation-dehydrogenation characteristic of Ti-6Al-2Sn-4Zr-6Mo. Accordingly, a comprehensive study was provided about the production of titanium powder from the Ti-6Al-2Sn-4Zr-6Mo secondary source by using the hydrogenation-dehydrogenation method in this thesis.

CHAPTER 2

THEORETICAL BACKGROUND

2.1 Titanium production

Titanium was discovered as an oxide in ilmenite ($FeTiO_3$) by William Gregor in 1791. Martin Heinrich Klaproth extracted titanium oxide from rutile (TiO_2) in 1795, and it was called “Titanium” based on Greek mythology, the Titans. Titanium production methods started to be established in the 1900s. Matthew Albert Hunter developed a process known as the Hunter process in 1940 (Hunter 1910) and the Kroll process which is still used today was developed by Wilhelm Justin Kroll who started the titanium industry metal in 1932 (Kroll 1940; Peters and Leyens 2003). Illustration of the Hunter and Kroll process is given in Figure 2.1. Both the Hunter and the Kroll processes begin with the preparation of the titanium tetrachloride ($TiCl_4$) from rutile which involves chlorination of TiO_2 and purification of $TiCl_4$. The reaction is given as

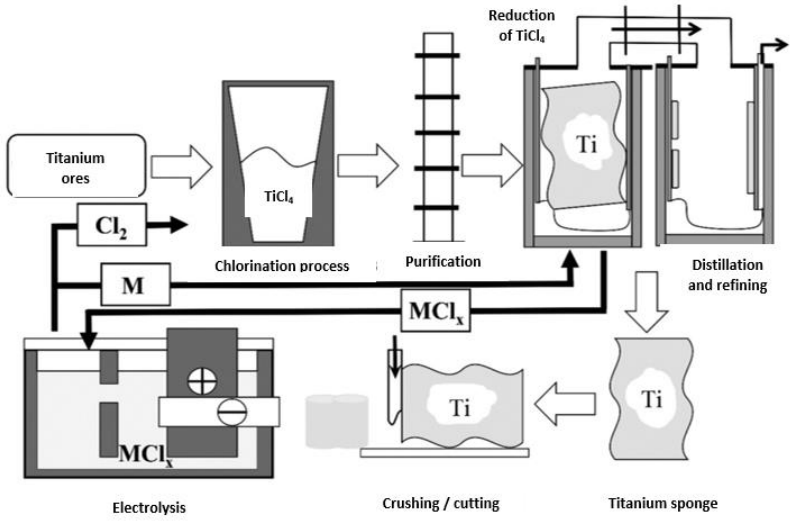

Figure 2.1. Illustration of the Kroll and Hunter processes
(Source: Song et al. 2020)

$$TiO_2(s) + 2Cl_2(g) + C(s) \rightarrow TiCl_4(g) + CO_2(g) \quad (1)$$

TiO_2 is heated up with chlorine gas and coke at 1030°C in a fluidized bed furnace (Takeda, Ouchi, and Okabe 2020). Some gases formed after the chlorination process such as $SiCl_4$ $FeCl_3$, excessive Cl_2, and CO_2 are removed to purify $TiCl_4$ by fractional distillation which is based on purification by boiling points (Sevryukov 1975).

Hata! Başvuru kaynağı bulunamadı. presents the differences and similarities b etween Kroll and Hunter processes. Titanium sponge production is based on reducing $TiCl_4$ by using different reductants. $TiCl_4$ is reduced by molten magnesium with argon gas in a steel chamber in the Kroll process (Fang et al. 2018; Nagesh, Ramachandran, and Subramanyam 2008). The reduction takes place at 750° C (Pehlke 1973) and $MgCl_2$ is produced as a by-product by the following reaction 2 (Kroll 1940) ;

$$TiCl_4(g) + 2Mg(l) \rightarrow Ti(s) + 2\,MgCl_2(l) \quad (2)$$

Moreover, magnesium and chlorine gas can be obtained by electrolysis of $MgCl_2$ and the resultant Cl_2 and magnesium can be used for the preparation and reduction of $TiCl_4$ respectively (Sevryukov 1975). Distillation is carried out to ensure removing excess $MgCl_2$ and magnesium from the titanium sponge.

$$MgCl_2(l) \rightarrow Mg(s) + Cl_2(g) \quad (3)$$

Molten sodium reacts with $TiCl_4$ over 800°C in the Hunter process (Hunter 1910). The same routes in the Kroll process are followed to produce titanium sponge. As seen in the reaction 4, 4 moles of sodium are required to obtain 1-mole titanium sponge, and NaCl is produced as a by-product that promotes obtaining high-quality titanium by preventing the contact of titanium with air (Florkiewicz et al. 2020).

$$TiCl_4(g) + 4Na(l) \leftrightarrow Ti(s) + 4NaCl(l) \quad (4)$$

Table 2.1. Comparison of Kroll and Hunter Process

	Kroll	**Hunter**
Feedstock	$TiCl_4$	$TiCl_4$
Reductant	Mg	Na
By product	$MgCl_2$	NaCl
Temperature (°C)	750	>800
Product	Sponge	Sponge with higher purity

Both Kroll and Hunter processes are known batch processes consuming time and energy. The purity of TiCl4 affects the purity of resultant titanium (Pehlke 1973) and iron is a common impurity found in these processes (Kohli 1981).

2.2 Titanium alloys and applications areas

Titanium and titanium alloys have found in several application areas owing to their exceptional properties, including corrosion resistance, low density, high strength to weight ratio, and biocompatibility These properties make them fascinating materials in biomedical, aerospace, maritime, chemical, and automotive industries as presented in Figure 2.2.

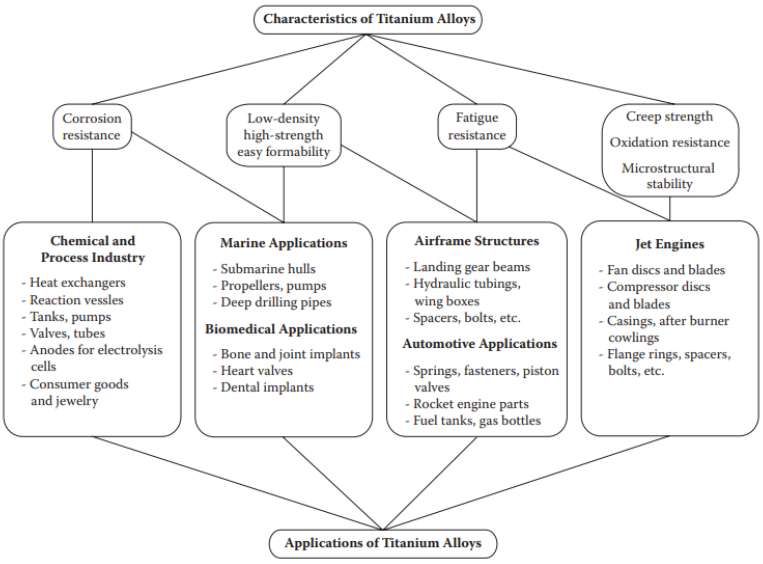

Figure 2.2. Characteristics of titanium alloys

(Source: Joshi 2006)

Titanium and its alloys have been one of the most preferred materials for the aerospace industry and have several advantages, as listed below, in comparison with aluminium, steel, and nickel-alloys (Williams and Boyer 2020).

- Weight savings
- High-temperature applications
- Space limitations
- Composites compatibility
- Low modulus

Due to their low density as well as excellent specific strength and availability at high temperatures, titanium alloys are widely used in engine and fuselage parts in this field. Also, crack propagation that may occur on the outer surface of the airframe is prevented by titanium alloys offer high fatigue resistance (Peters et al. 2003).

Besides the aerospace industry, titanium alloys have found prevalent applications owing to their corrosion resistance, biocompatibility, and low density in nonaerospace fields such as biomedical, chemical, petrochemical, marine, and military industries (Gurrappa 2003).

Biomaterials must exhibit many main properties, namely high corrosion resistance, osseointegration, excellent wear resistance, and good mechanical properties (de Viteri and Fuentes 2013). Hence, Commercially Pure Titanium (CP-Ti) and β-titanium alloys are used as biomaterials in orthodontics and orthopaedics applications, as they offer high biocompatibility, good corrosion resistance, low density, and Young's moduli (Simona Baltatu et al. 2019).

It is intended to reduce fuel consumption by weight reduction, a priority in the automobile industry (Froes et al. 2004). Thus, the system performs better and gains environmentally friendly characteristics. From this point of view, titanium alloys have found use in the automobile industry, especially in producing suspension springs and engine components (Sherman and Allison 1986).

2.3 Properties of Titanium

Titanium is the heaviest light metal (4.51 g /cm^3) with different crystal structures, including hexagonal close-packed structure (hcp) and body-centered cubic structure (bcc), which are also referred to as alpha (α) and beta (β) phases as seen in Figure 2.3, are stable within particular temperatures. (Veiga, Davim, and Loureiro 2012).

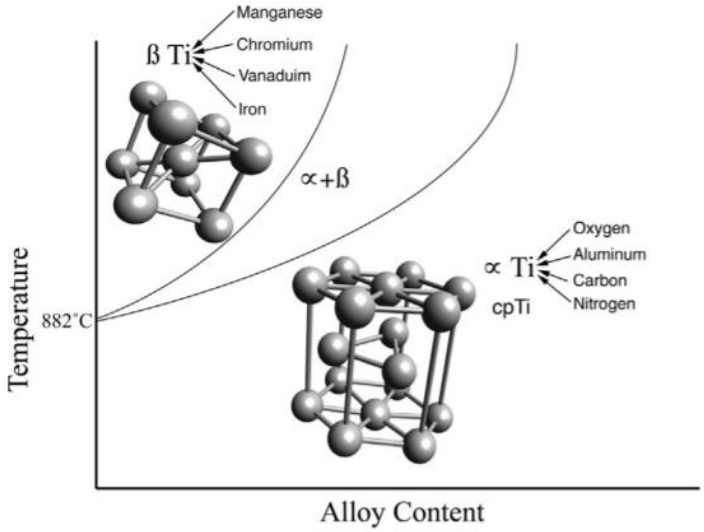

Figure 2.3. Crystal structure of α and β titanium
(Source: Prasad et al. 2015)

α phase exists at lower temperatures however, allotropic transformation occurs at 882 °C, where the β phase is stable (Joshi 2006). It is one of the transition elements with incomplete shells in the IV group. That's why titanium has a high potential to make solid solution with other elements (Joshi 2006). Some characteristics of pure titanium are tabulated in Table 2.2. Pure titanium has a high melting point of 1670 °C. Also, it has low modulus and thermal conductivity.

Table 2.2. Properties of pure Titanium
(Source: Lutjering &Williams 2007)

Property	Value
Atomic number	22
Atomic weight	47.9
Density g/cm^3	4.51
Melting Point °C	1670
Boiling Point °C	3260
α to β transus °C	882

2.4 Titanium alloys

Different kinds of titanium alloys are classified as α titanium alloys, α-β titanium alloys, and β titanium alloys by alloying elements. These elements improve the properties of titanium and extend application areas of materials and can be categorized as neutral, α stabilizer, and β stabilizer as shown in Figure 2.4.

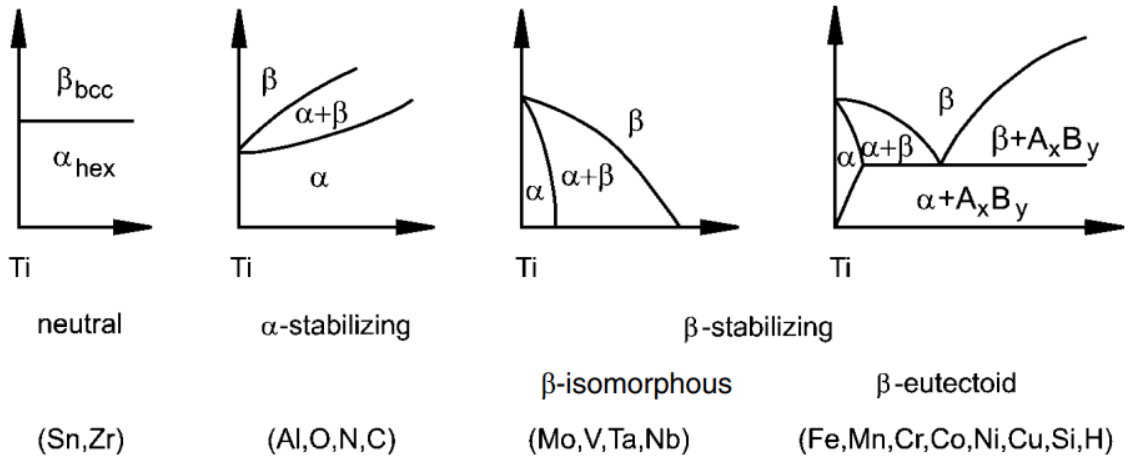

Figure 2.4. Phase diagrams of titanium alloys according to the different kinds of stabilizer (Source: Peters and Leyens 2003)

2.4.1 The α titanium alloys

Aluminum, oxygen, carbon, and nitrogen are known as α stabilizer found in α titanium alloys. Expansion of the α phase to high temperature is promoted by these elements (Peters and Leyens 2003). The α titanium alloys are categorized as unalloyed, α alloy, and near α titanium alloy (Weiss and Semiatin 1999). CP-Ti is also known as an unalloyed α alloy that differs in the amount of oxygen (O) and iron (Fe) with low tensile strength (Weiss and Semiatin 1999). Near α alloys allow working at high temperatures up to 550 °C with 1-2 % of β stabilizer molybdenum or/and vanadium (Peters and Leyens 2003). α titanium alloys can be welded, although they are not heat treatable (Titanium Alloys - Novel Aspects of Their Manufacturing and Processing 2019). They have found applications in the chemical, process engineering industries, and elevated temperature applications. The most used α alloys tabulated in Table 2.3 are CP-Ti, Ti-0.2Pd, Ti-0.3Mo-0.8Ni, Ti-5Al-2.5Sn, and Ti-3Al-2.5V. Ti-0.2Pd and Ti-0.3Mo-0.8Ni have better corrosion resistance compared with CP-Ti (Boyer 1996). Ti-3Al-2.5V alloy is called “Half Ti-6-4” and is widely used in aircraft systems and sporting goods (Bolzoni, Ruiz-Navas, and Gordo 2012; Lutjering and Williams 2007).

Table 2.3. Important commercial α titanium alloys
(Source: Lutjering &Williams 2007)

α alloys and CP-Ti	**Alloy Composition (wt%)**
Grade 1	CP-Ti (0.2Fe, 0.18O)
Grade 2	CP-Ti (0.3Fe, 0.25O)
Grade 3	CP-Ti (0.3Fe, 0.35O)
Grade 4	CP-Ti (0.5Fe, 0.40O)
Grade 7	Ti-0.2Pd
Grade 12	Ti-0.3Mo-0.8Ni
Ti-5-2.5	Ti-5Al-2.5Sn
Ti-3-2.5	Ti-3Al-2.5V

2.4.2 The β titanium alloys

β stabilizer elements are divided into isomorphous and eutectoid used 30% in β titanium alloys (Bania 1994; Joshi 2006). Molybdenum, vanadium, tungsten, niobium, and tantalum are isomorphous β-stabilizers, and iron, chromium, copper, nickel, cobalt, manganese, and sulphur are eutectoid β-stabilizers that strengthen the β phase and decrease β transus temperature (Cotton et al. 2015). Some commercial β titanium alloys are given in Table 2.4. These alloys exhibit high strength-to-weight ratio, low elastic modulus, low toxicity and are preferred in many fields, including aerospace, power plant, sporting goods, automotive, and orthopaedic implants (Weiss and Semiatin 1998).

Table 2.4. Important commercial β titanium alloys
(Source: Lutjering &Williams 2007)

β Alloys	**Alloy Composition (wt%)**
Ti-17	Ti-5Al-2Sn-2Zr-4Mo-4Cr
SP-700	Ti-4.5Al-3V-2Mo-2Fe
Beta-CEZ	Ti-5Al-2Sn-2Cr-4Mo-4Zr-1Fe
Ti-10-2-3	Ti-10V-2Fe-3Al
Beta 21S	Ti-15Mo-2.7Nb-3Al-0.2S
Ti-LCB	Ti-4.5Fe-6.8Mo-1.5Al
Ti-15-3	Ti-15V-3Cr-3Al-3Sn
Beta C	Ti-3Al-8V-6Cr-4Mo-4Zr
B120VCA	Ti-13V-11Cr-3Al

2.4.3 The α-β titanium alloys

Molybdenum, vanadium, tungsten, tantalum, and silicon are known as β stabilizer elements which stabilize β phase in titanium alloys at room temperature. α-β titanium alloys provide high tensile and fatigue strength, high corrosion and creep resistance, and good hot formability. These alloys have been widely used for producing of sailoring components and most parts used in aerospace like steam turbine blades, blades and discs of aircraft turbines (Titanium Alloys - Novel Aspects of Their Manufacturing and Processing 2019). Common α-β titanium alloys are listed in

Table 2.5. Among titanium alloys, Ti-6Al-4V (Ti-64) is the most preferred α-β titanium alloy which is widely used in titanium markets. Ti-6Al-2Sn-4Zr-6Mo is

another α-β alloy that has found application in the aerospace field due to its high fatigue strength and toughness at 315–400°C (Hassanin et al. 2021). It is used for the manufacturing of compressor discs, turbine blisks, spacers and gaskets.

Table 2.5. Common commercial α-β titanium alloys
(Source: Lutjering &Williams 2007)

α -β Alloys	**Alloy Composition (wt%)**
Ti-811	Ti-8Al-1V-1Mo
IMI 685	Ti-6Al-5Zr-0.5Mo-0.25Si
IMI 834	Ti-5.8Al-4Sn-3.5Zr-0.5Mo-0.7Nb-0.35Si-0.06C
Ti-6242	Ti-6Al-2Sn-4Zr-2Mo-0.1Si
Ti-6-4	Ti-6Al-4V (0.20O)
Ti-6-4 ELI	Ti-6Al-4V (0.13O) 975 Ti-662 Ti-6Al-6V-2S
IMI 550	Ti-4Al-2Sn-4Mo-0.5Si
Ti-6246	Ti-6Al-2Sn-4Zr-6Mo

2.5 Titanium secondary sources

Despite the outstanding properties of titanium alloys, they are referred as difficult-to-cut materials (Che-Haron 2001). This arises from their low thermal conductivity, low modulus of elasticity, and high chemical reactivity (Gao, Wang, and Liu 2016). Besides, the high melting point, extraction process, and high oxygen affinity of titanium increase the production cost (Festas, Ramos, and Davim 2022). Therefore, challenges in the machining of titanium should be minimized because machining methods including milling, reaming, tapping, sawing, and grinding are still used to produce titanium parts (Ezugwu and Wang 1997) and a large amount of machining waste is generated during these operations.

Titanium scraps are classified into three groups: mill scrap, fabrication scrap, and recycled scrap. Scraps generated in processes such as melting, forging and rolling are considered as the mill scrap. Fabrication scrap is generated during the production and shaping of titanium parts and scrap from old heat exchangers, aircraft or other equipment is also known as recycled scrap.

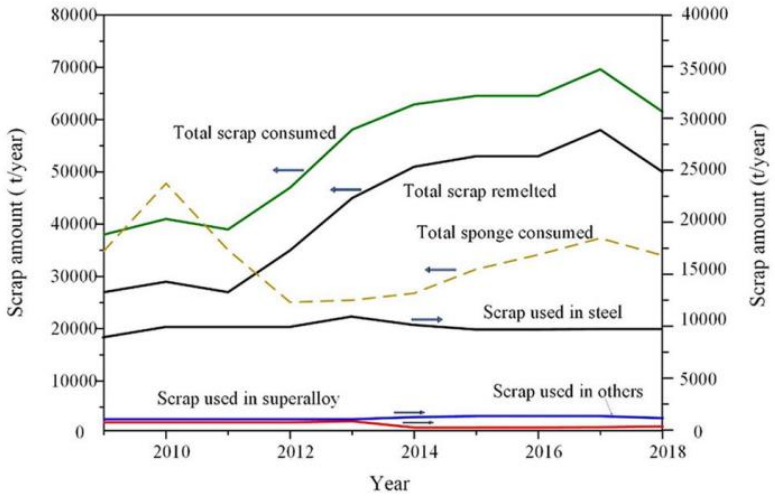

Figure 2.5. Statistic based on the production titanium-based scrap and use in the USA between 2009 and 2018 (Source: Xia et al. 2019)

The amount of titanium scrap has been increasing each year (Xia et al. 2019) as shown in Figure 2.5 (USGS statistics). Buy to fly ratio is the weight ratio between the amount of raw material used to manufacture a component and the amount of the final part in aerospace industry (Caiazzo et al. 2017) and this value is 12.2:1 for manufacturing F-22 jet. It refers only 18% of titanium can be used as raw material and rest of them are scrap (Fang et al. 2018). As presented in Table 2.6, extraction and processing cost of titanium are much higher than its competing materials like steel and aluminium (Froes et al. 2004). That is why recycling technologies should be a prime concern considering titanium cost and its scrap generation. Also, by contributing to recycling, limited natural resources can be protected, energy saving and contribution to the economy can be promoted. Moreover, CO_2 emissions can be reduced by approximately 95% by recycling (Sohn 2021).

Table 2.6. Comparison of Cost of Steel, Aluminium and Titanium (Source: Faller and Froes 2001)

Item	**Material ($ per pound)**		
	Steel	**Aluminium**	**Titanium**
Ore	0.02	0.10	0.30
Metal	0.10	0.68	2.00
Ingot	0.15	0.70	4.50
Sheet	0.30 - 0.60	1.00 - 5.00	15.00 – 50.00

Cold hearth melting (CHM) and vacuum arc re-melting (VAR) are widely used for recycling Ti scraps in industry (Pan et al. 2019). Both VAR and CHM processes are known as consolidation processes where titanium ingot is produced by using titanium sponge or titanium scrap (Truong et al. 2022). However, these processes are high cost since these techniques are based on melting metal. Both processes are designed to protect molten titanium from air.

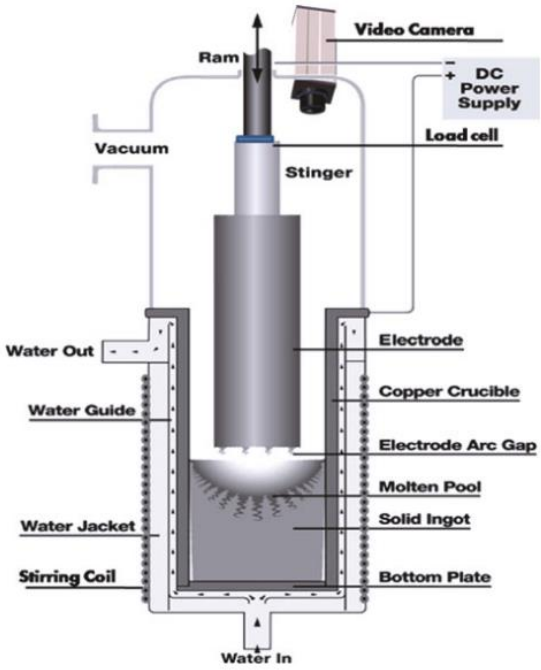

Figure 2.6. Sketch of the VAR process
(Source: Woodside, King, and Nordlund 2013)

Compacted feedstock which is referred to as an electrode is melted by plasma arc in VAR process (Alam, Semiatin, and Ali 1998). Melting process can be repeated more than once to increase homogenization of final product. As presented in Figure 2.6 water jacket covers copper crucible for cooling the melt and controlling the solidification rate.

Electron beam guns or plasma torches can be used to obtain molten material in CHM process (Williams and Boyer 2020). Vacuum atmosphere is required in electron beam cold hearth melting while argon is required in plasma arc melting (Lutjering and Williams 2007). Molten material flows along the water-cooled copper melting hearth as seen in Figure 2.7 and inclusions can be removed or dissolved according to their densities (Truong et al. 2022). Then, the molten metal is solidified to obtain ingot.

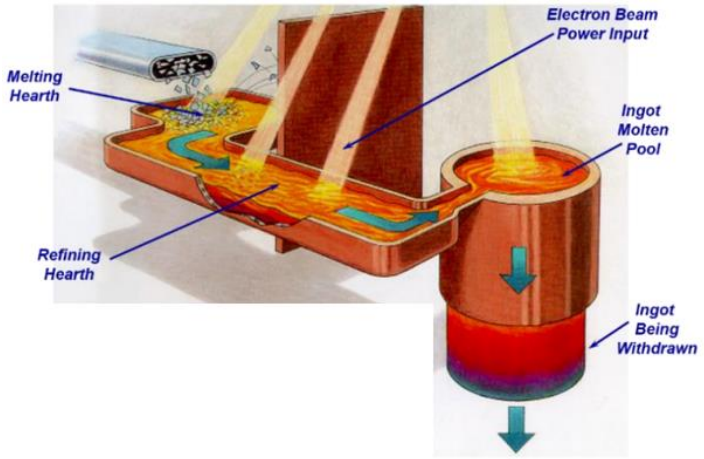

Figure 2.7. The cold hearth melting unit
(Source: Lutjering and Williams 2007)

2.6 Titanium powder metallurgy

The expansion of various industrial fields has allowed the development of powder metallurgy (P/M), where cost reduction with little waste is a prime goal (Tsutsui 2012). This cost-effective route involves powder production, compaction, shaping, and sintering processes as presented in Figure 2.8 (Sam Froes 2015; Lutjering and Williams 2007). Moreover, it has great potential to reduce the amount of scrap produced (Fang et al. 2018).

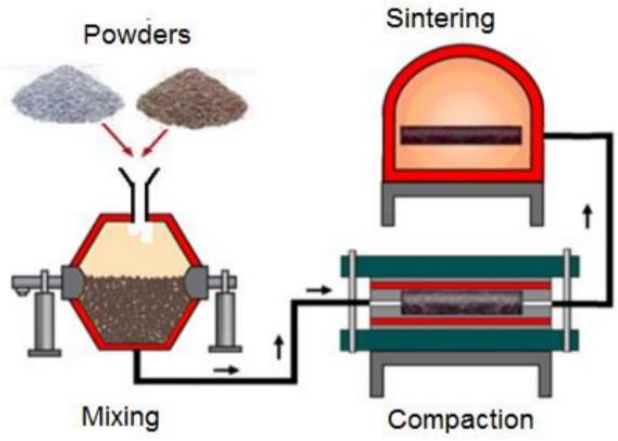

Figure 2.8. Production of bulk products by using powder metallurgy
(Source: Hamweendo, Malama, and Botef 2016)

P/M of titanium was established in the 1980s and has two approaches, including pre-alloyed (PA) and blended elemental (BE) methods (Fujita et al. 1996). Comparing BE and PA techniques, the production cost of BE is lower. Titanium powders have been widely used in many processes such as metal injection moulding (MIM) and hot isostatic pressing as well as in additive manufacturing (AM) techniques like selective laser melting (SLM), electron beam melting (EBM), and directed energy deposition (DED) (P. Sun et al. 2017), which have received increasing attention in the global industry (Qian and Bourell 2017; L. Chen et al. 2017). There several of conventional titanium powder production methods. Atomization technique is well known process which demands a large infrastructure and production cost. The following methods are used as alternatives which aim a cost reduction: Armstrong, Fray-Farthing-Chen (FCC) Cambridge, and HDH processes.

2.6.1 Atomization

Atomization is highly advanced method where the metal is liquefied, then molten titanium is atomized, and lastly cooled to produce spherical titanium powder (P. Sun et al. 2017). Atomized powders can be widely used in AM because of their shape. However, there are some limitations, including high cost and having wide particle size distribution for atomization techniques. There are different types of atomizing techniques including plasma rotating electrode process (PREP), gas atomization (GA), electrode induction melting–gas atomization (EIGA), and plasma atomization as shown in Figure 2.9.

Pre-alloyed materials such as rods, ingots, and alloys are chosen to melt in the crucible under a vacuum atmosphere in GA (Moll 2000). The molten material can be held for a while to ensure that the homogenization of the melt is complete. Afterwards molten metal is transferred into the nozzle and atomized with argon gas. There are two different techniques in GA including free-fall gas atomization (FFGA) and close-coupled gas atomization (CCGA) (Jang et al. 2020). Gravity forces promote the downward movement of droplets before atomization in FFGA. These two techniques differ from each other in terms of the size of the produced powder and finer particles can be obtained by CCGA.

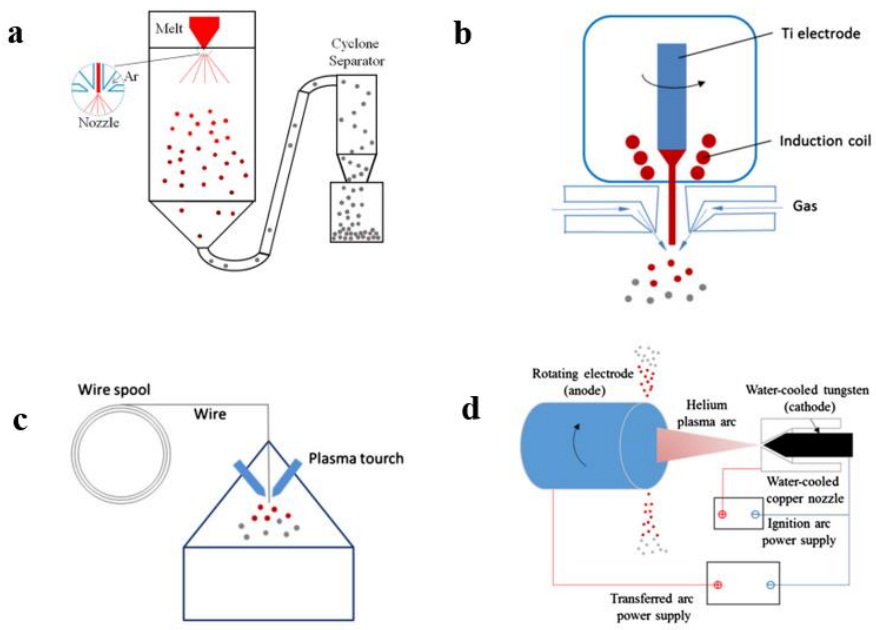

Figure 2.9. Schematic diagrams for (a)gas atomization (GA), (b) electrode-induction gas atomization (EIGA) (c) plasma atomization (PA) (d) plasma rotating electrode process (PREP) (Source: Fang et al. 2018)

In EIGA, a pre-alloyed rod is used as feedstock placed in a conical induction coil (Gerling, Clemens, and Schimansky 2004). Slow rotation of the electrode around its symmetry axis enhances the homogenization of melt (Spitans, Franz, and Baake 2020). Melting starts from the tip of the rod and molten material is collected to atomize in the gas nozzle with argon gas. The EIGA process results in solidifying the molten droplets going down the atomization tower. High purity powders, as well as spherical-shaped, are produced with small electric power, and the size distribution of EIGA powder depends on the diameter of the rod.

Titanium wire is heated up by plasma torch which melts the material with high velocity in PA (Entezarian et al. 1996). Fine droplets are solidified around 100-1000 °Cs $^{-1}$ cooling rate in the argon atmosphere (Jang et al. 2020). PA powders are produced with high-quality spherical-shaped and offer narrower size distribution, around 40 μm, compared to gas atomization and rotating electrode processing (Entezarian et al. 1996).

The PREP process is known as an advanced version of the rotating electrode process (REP) (Nachtrab, Roberts, and Newborn 1992). The helium plasma arc is used instead of the tungsten arc cathode to melt electrode rod and centrifugal forces promote

obtaining molten droplets in stainless steel chamber (Roberts 1989; P. Sun et al. 2017). PREP powders are produced in wide range of particle sizes as 50-300 μm with high purity. Electrode diameter and rotational speed affect particle size distribution of powder.

2.6.2 Armstrong process

High purity titanium and titanium alloy powders are produced in one step by the Armstrong process which is known as a cost-effective version of the Hunter process (Wei Chen, Yamamoto, and Peter 2010; W. Chen et al. 2011). This process is based on reducing the metal halide to titanium powder as seen in the reaction 5 (Imam and Froes 2010).

$$TiCl_4(g) + 4Na\ (1) \rightarrow Ti(s) + 4NaCl(s) \quad (5)$$

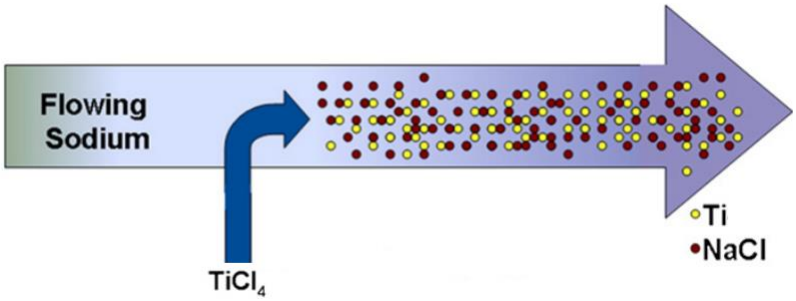

Figure 2.10. Illustration of the Armstrong Process

(Source: W. Chen et al. 2011)

Vapor of $TiCl_4$ is introduced into the system with a following liquid sodium at a single point and it leads to complete reaction at a lower temperature and reduces the size of titanium particles (Crowley 2003). The NaCl formed as a result of this reaction is removed by washing to obtain dendritic “coral-like” titanium powder directly.

2.6.3. Fray-Farthing-Chen (FFC) Cambridge process

The Fray-Farthing-Chen (FFC) Cambridge process is an electrochemical reduction process where titanium is extracted from solid TiO_2 in molten $CaCl_2$ (Schwandt, Doughty, and Fray 2010). This process offers a low-cost approach considered an alternative to the Kroll process (Ma et al. 2006).

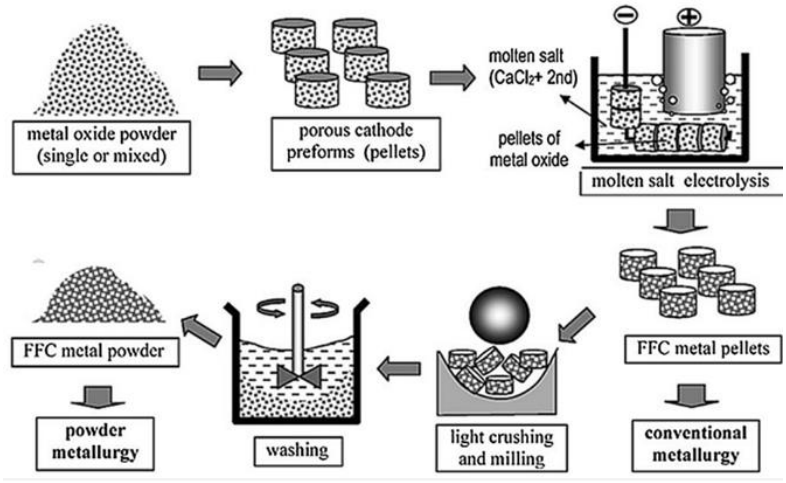

Figure 2.11. An illustration of the FFC-Cambridge process
(Source: Hu et al. 2018)

The electrolytic cell consists of the pressed TiO_2 powder used as a cathode, carbon-based or inert anode, and $CaCl_2$ electrolyte (D. Wang, Jin, and Chen 2008). Porous TiO_2 cathode enhances reaction rate with increasing surface area (Larminie and Dicks 2003). Voltage which decomposes cathode but does not decompose molten $CaCl_2$ is applied, to separate oxygen from TiO_2. The cathodic and anodic reactions in this process are shown in the following reaction 6,7,8 and 9 (Centeno-Sánchez, Fray, and Chen 2007; Fray 2016)

cathodic reaction;

$$TiO_x + 2xe^- = Ti + xO^{2-} \quad (6)$$

anodic reaction when inert anode is used

$$xO^{2-} = (x/2)O_2(g) + 2xe^- \quad (7)$$

when graphite anode used

$$xC + xO^{2-} = xCO + xe^- \quad (8)$$

$$x/2C + xO^{2-} = x/2CO_2 + xe^- \quad (9)$$

Graphite is often used as an anode and a reaction occurs between stripped oxygen and graphite to form CO to supply energy to the system(Centeno-Sánchez, Fray, and Chen 2007; Schwandt 2013). Moreover, O_2 gas is released when an inert anode is

chosen. To obtain titanium powder, reduced metal on the cathode is washed to remove the salt.

2.6.4 Hydrogenation-Dehydrogenation (HDH) process

The HDH process was established to produce titanium powder at the Titanium Metals Corporation in 1957s (Barbis et al. 2015). HDH is a solid-state process where a substance is exposed to hydrogen at a specific temperature and pressure, and then hydrogen is removed by vacuum and/ or thermal treatment (Dunstan et al. 2019). There are three main steps in this process: hydrogenation, milling (size reduction), and dehydrogenation. The primary purpose of the hydrogenation is to obtain Titanium hydride powder which is considered as a brittle intermediate product (C. Wang et al. 2016). Hydrogenation promotes embrittlement and thus powder production.

In general, metal hydrides are formed by the reaction of hydrogen with the metal and metal alloys following the reaction 10 (Mitkov and Božić 1996);

$$M + x/2H_2 \leftrightarrow MH_x + Q \quad (10)$$

In this equation, M and Q represent metal and heat of reaction, respectively. This reaction is a reversible reaction. and the direction of reaction depends on whether hydrogen gas pressure is above the equilibrium pressure (Mitkov and Božić 1996). When hydrogen pressure is above equilibrium pressure, metal hydride can be easily obtained with heat of formation. That's why the metal hydride formation is an exothermic reaction.

Hydrogen can react with titanium, thereby modifying both its crystal structure and mechanical properties (Z. Sun et al. 2009). Titanium hydride formation enhances crack propagation and fragmentation. After hydrogen charging on the titanium matrix, the next step is milling for powder production. The resulting powders can be sieved and classified to the desired particle sizes. Hydrogen is removed under a certain temperature and vacuum to obtain titanium powder in the last step, dehydrogenation. Furthermore, the removal of hydrogen is an endothermic reaction.

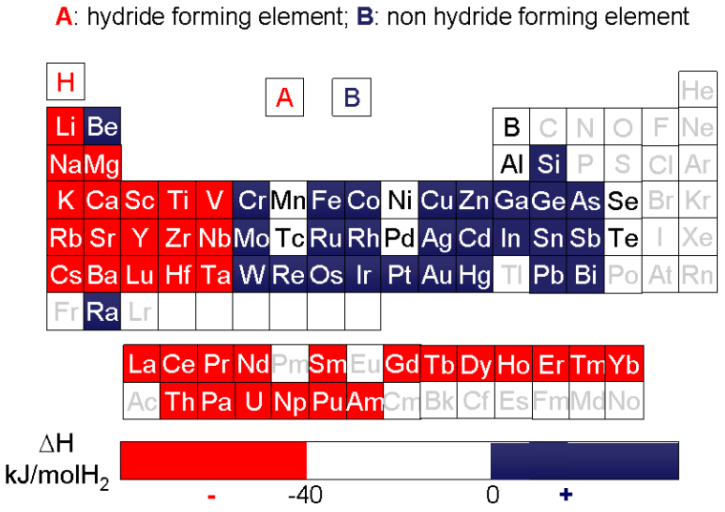

Figure 2.12. Hydride formation characteristic of elements
(Source: Thermodynamics – Interaction Studied – Solids,Liquids and Gases 2012)

HDH process is also widely preferred in recycling technologies. Many studies have been conducted on the recycling of titanium by using this technique in literature. In research from Umeda et al. (2017), Ti-64 powder was obtained from Ti-64 chips by using the HDH process. Hydrogenation conditions were tried to be optimized and the effect of hydrogenation on milling was examined. Moxson et al. (2002) synthesized CP-Ti and Ti- 64 powders from their turnings with acceptable impurity levels. Oh et al. (2014) revealed that high-quality Ti-Mo and Ti–V powders could be obtained by using the HDH process and additional routes such as deoxygenation. Gökelma et al. (2018) assessed the utility of recycled Ti-64 powders in the additive manufacturing field.

2.7 Comparison of the powder metallurgy methods

Most of the titanium powder production methods are costly. Atomization techniques are based on melting titanium metal. Because of its high melting point and oxygen affinity, inert environment must be provided to obtain high-quality products. In the FFC process, TiO_2 should be extracted from its ores with high purity. Therefore, all these processes increase the production cost. Among them, the HDH process has gained more attention as a cost-effective method. Since it is based on solid-state reaction and scrap can be used as a feedstock only in HDH process as tabulated in Table 2.7.

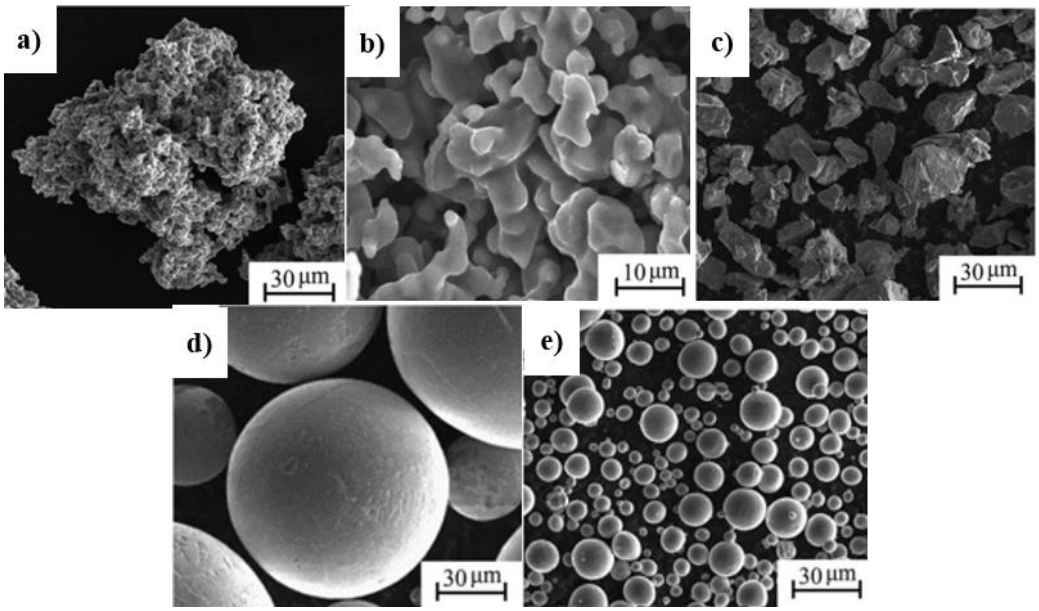

Figure 2.13. SEM images of Titanium powders by different processes (a) Armstrong, (b) FFC (c) HDH (d) PREP and (e) PA (Source: Fang et al. 2018)

It is seen in Figure 2.13 that the morphology of the powders produced also differs from each other. While spherical powders are obtained in atomization techniques, non-spherical powders are obtained in HDH, Armstrong, and FFC processes. The usage of non-spherical powders is restricted in some areas, such as additive manufacturing, because of their low flowabilities.

Table 2.7. Comparison of titanium powder production methods (Source: Fang et al. 2018)

Methods	**Feedstock**	**Reductant**	**By-products**	**Product**	**Morphology of the product**
Armstrong	$TiCl_4$	Na	NaCl	Powder	Non-spherical
Atomization	Rod, wire, ingot	-	-	Powder	Spherical
FFC	TiO_2	Applied current	CO, CO_2 (from carbon anode)	Pellets/powder	Non-spherical
HDH	Primary or secondary metal alloy	-	-	Powder	Non-spherical

2.8 Mechanism of hydrogen diffusion in Titanium matrix / of Titanium hydride formation

Titanium and its alloys exhibit high hydrogen affinity and Titanium hydride can be easily formed when titanium is exposed to hydrogen gas as indicated in reaction 10. Figure 2.14 demonstrates the stages that follow each other in order for the metal hydride formation.

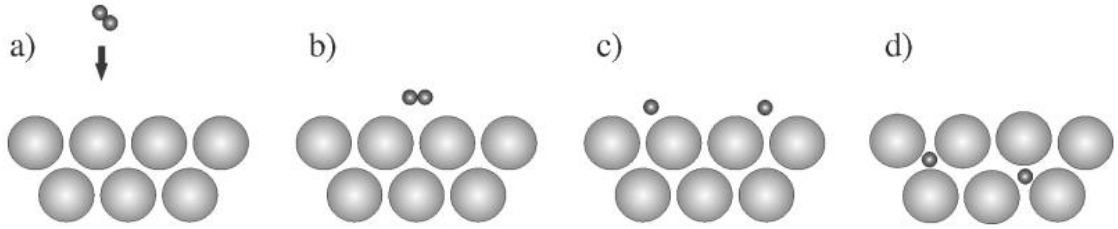

Figure 2.14. The reaction of H_2 molecule with a storage material a) H_2 molecule approaching the metal surface. b) Physisorption c) Chemisorption d) Hydrogen diffusion (Source: Thermodynamics – Interaction Studied – Solids,Liquids and Gases 2012)

Hydrogen molecules are directed to the metal surface by the Van der Waals forces that promote interaction of atoms on the solid surface and hydrogen gas molecules (Züttel 2003). This phenomenon is called physisorption and chemisorption is the following step where hydrogen molecules dissociate for forming a metal-hydrogen bond (Thermodynamics - Interaction Studies - Solids, Liquids and Gases 2012).

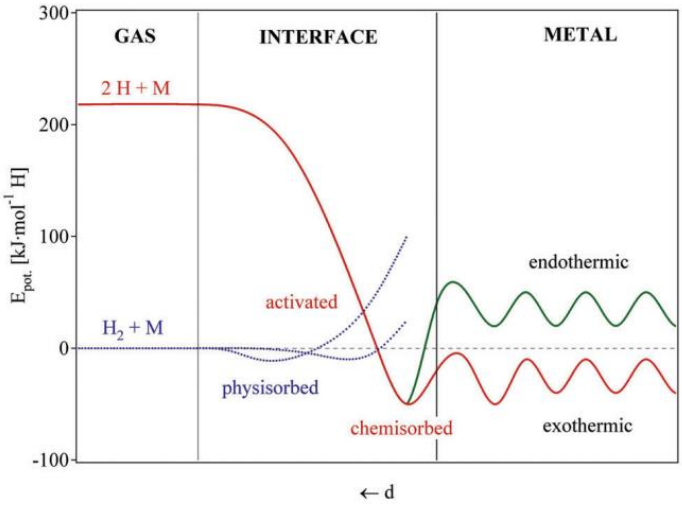

Figure 2.15. Comparison of potential energies of molecular and atomic hydrogen when interaction with metal (Source: Züttel 2003)

The activation energy required for this dissociation is reached at this stage as seen in Figure 2.15. After dissociation on the metal surface, the H atoms diffuse to form M-H solid solution into the bulk which leads to lattice expansion as seen in Table 2.8 (Thermodynamics - Interaction Studies - Solids, Liquids and Gases 2012).

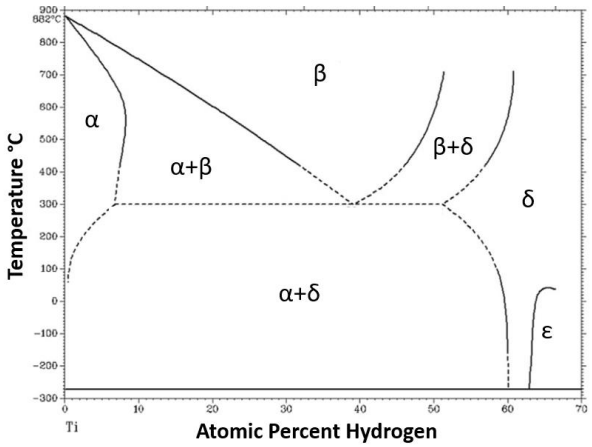

Figure 2.16. Phase diagram for the Ti–H system (Source: San-Martin and Manchester 1987)

Hydrogen stabilizes the β phase and reduces the allotropic transformation temperature to approximately 300°C as presented in Figure 2.16. As the hydrogen concentration increases in the titanium-based matrix, different hydrides such as α, β, γ, δ and ε are formed with different lattice type both as seen in Table 2.8 and Figure 2.16 (Numakura et al. 1986). δ hydride with fcc structure (CaF2 type) includes compositions

TiHX, where x in the range $1.5 \leq x \leq 1.99$.When x is higher than 1.99, ε hydride with fct structure exists (Wu and Wu 2002).

Table 2.8 Types of Titanium-Hydrides

Phase	**α**	**β**	**γ**	**δ**	**ε**
Lattıce type	hcp	bcc	fct c<a	fcc c=a	fct c>a
Lattice parameter, Å	a=2.95 c=4.69	a=3.305	a=4.21 c=4.6	a=4.4	a=4.5 c=4.3
Hydrogen concentration range	0-10	10-44	44-50	50-66	66-67
Phase formula	$TiH_{0.1}$	$TiH_{0.3}$	TiH	$TiH_{1.5}$	TiH_2

The solubility and diffusion of hydrogen in titanium depend on several variables such as temperature, pressure, alloy composition, chemical purity, etc. (Wasz et al. 1996). Comparing β-titanium and α-titanium, β-titanium promotes hydrogen solubility and a higher diffusion rate because α-titanium has more closed packed structure where atomic packing factor value is 74%, compared to 64% for β-titanium. According to the following equations 11 and 12;

$$D_\alpha = 1.8\, x\, 10^{-6}\, exp\left(\frac{-6230}{T}\right) \quad (11)$$

$$D_\beta = 1.95 \text{ x } 10^{-7} \exp\left(\frac{-3342}{T}\right) \quad (12)$$

where Dα is the diffusivity of hydrogen in the α phase, Dβ is the diffusivity of hydrogen in the β phase and T is the temperature (Luo et al. 2006). This arises from 12 tetrahedral and six octahedral interstices in the β phase. α phase consists of only 4 tetrahedral and 2 octahedral interstitial sites (Tal-Gutelmacher and Eliezer 2004).

Considering the passivation layer of titanium, hydrogen absorption is inhibited by this layer. This can arise from different hydrogen diffusion coefficients of TiO_2 (rutile) and pure α- titanium that are 7.5 x 10^{-20} $cm^2\ s^{-1}$ and 1.07 x 10^{-12} $cm^2\ s^{-1}$ at 20°C respectively. Moreover, hydrogen diffusivity can be influenced by the temperature, chemical composition and structure of surface layer, types of impurities, etc.

2.9 Oxidation behaviour of Titanium

Like hydrogen and nitrogen, oxygen also has high solubility in titanium-based matrix at elevated temperature and this always results in the formation of a passive layer on metal surface within few seconds that prevents metal from further oxidation (Gemelli and Camargo 2007). Furthermore, oxygen diffusion zone which exhibits brittle characteristic is referred as crucial zone because of modifying both mechanical properties and crystal structure of alloys.

Figure 2.17 presents Ellingham diagram showing the formation of different metal oxides and formation of titanium oxide is thermodynamically favourable than lots of metal oxides except aluminium and calcium oxides.

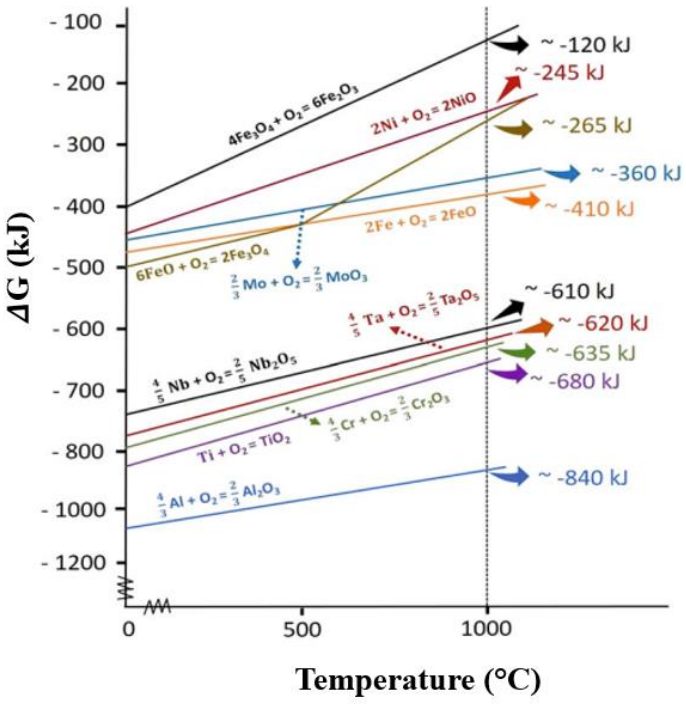

Figure 2.17. Ellingham diagram

Titanium oxides form when oxygen precipitates with different concentrations in titanium matrix including TiO, Ti_3O, Ti_2O_3. TiO_2 as seen in Figure 2.18. Titanium and its alloys exhibit high oxygen solubility up to 40% by weight. Most stable titanium oxide is TiO_2 which has tetragonal crystal structure with highest oxygen concentration as 40.03 %.

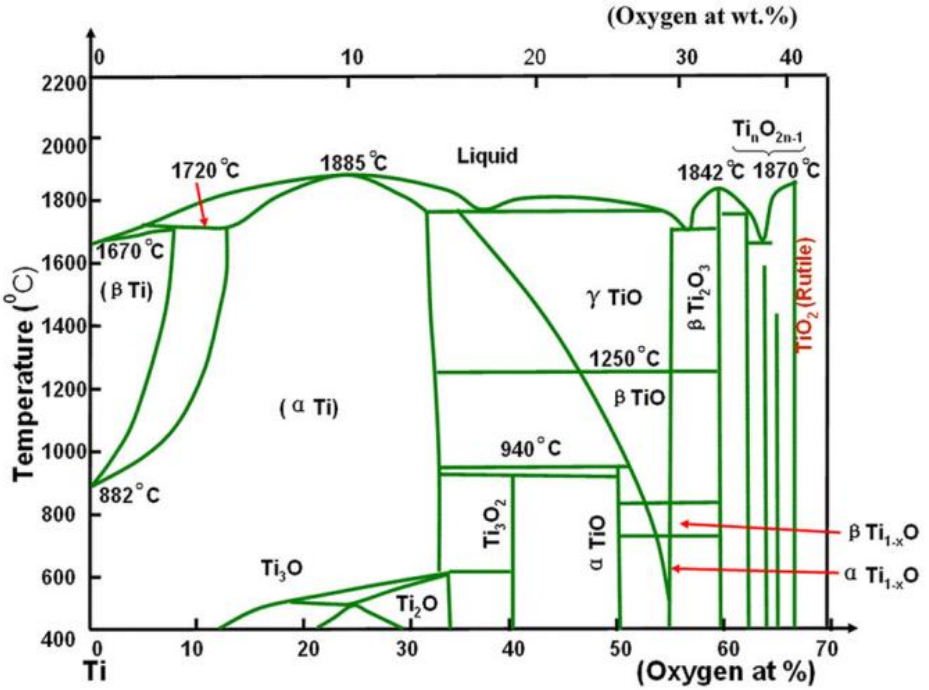

Figure 2.18. Ti-O phase diagram

Characteristics of titanium oxides are tabulated in Table 2.9 that increasing oxygen content promotes change in crystal structure and colour.

Table 2.9. Types of Titanium oxides (Source: Xia et al. 2019)

Oxide state		**Oxygen (wt%)**	**Crystal structure**	**Colour**
Magneli Phases	TiO_2	40.03	Tetragonal	White
	Ti_nO_{2n-1}	37.5-36.8	Triclinic	
High Ti-containing oxide	Ti_3O_5	35.75	α, β, γ monoclinic	α -dark blue γ-dark red
	Ti_2O_3	33.36	β, α phase	Purple
	TiO_x $0.7<x<1.3$	20.7-11.2	α, β or γ ccc	γ -Gold
Solid solution	TiO_x $x<0.7$	<11.2	α	Silver

Titanium oxides with different oxygen content offer different colour scale for several applications like TiO_2 is widely used as pigment in coating industry. It has been documented from previous work TiO_2 and TiO were white and golden tinted, respectively, Ti_2O_3 and Ti_3O_5 were blue coloured and dark violet, respectively.

CHAPTER 3

EXPERIMENTAL WORK

3.1 Materials

Titanium sponge and Ti-6Al-2Sn-4Zr-6Mo turnings were received from Zirom S.A. Magnesium chips were supplied from Kar Mineral Madencilik to lower the oxygen content of the atmosphere at high temperatures. Chemical composition of Ti-6Al-2Sn-4Zr-6Mo and Magnesium chips are tabulated in Table 3.1 and Table 3.2. High purity (99.999 %) H_2 and Ar-H_2 (95 % Ar + 5% H_2) were supplied from Linde and they were used for the hydrogenation of turnings. High purity (99.999 %) Argon was supplied from Linde for cleaning the HDH reactor. Acetone (> 99.5 %) was supplied from Tekkim Kimya for cleaning the cutting oil on turnings. The deionized water (18.2 MΩ•cm−1 at 25 °C) was supplied by using a Milli-Q Advantage water treatment system.

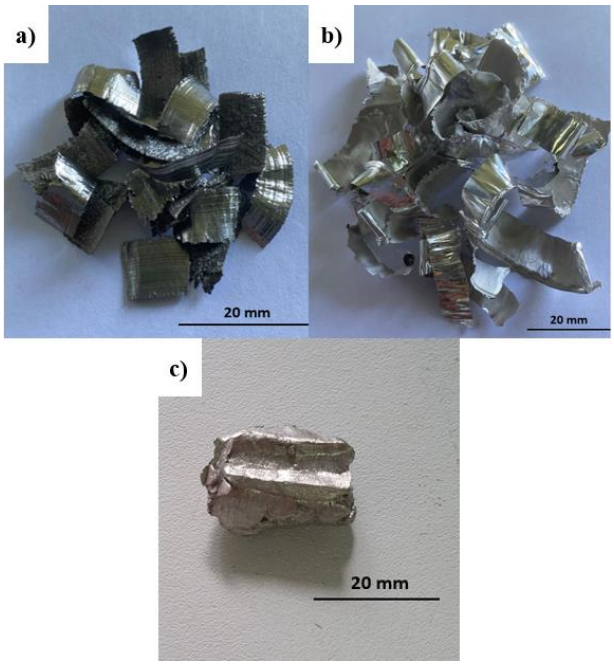

Figure 3.1. a) Ti-6Al-2Sn-4Zr-6Mo turnings b) Pure Magnesium chips c) Titanium sponge

Table 3.1. Chemical Composition (%) of Ti-6Al-2Sn-4Zr-6Mo

Al	**Mo**	**Zr**	**Sn**	**Fe**
5.82	5.82	4.04	2.13	0.116
C	**O_2**	**N_2**	**H_2**	**Ti**
0.015	0.110	0.008	0.003	Balanced

Table 3.2. Chemical Composition (%) of Magnesium Chips

Mg	**Be**	**Fe**	**Ca**	**Mn**	**Al**
99.96	0.0001	0.0038	0.0005	0.0181	0.0045
Ni	**Cu**	**Zn**	**Na**	**Si**	
0.0005	0.0019	0.0033	0.0011	0.0048	

3.2 Equipment

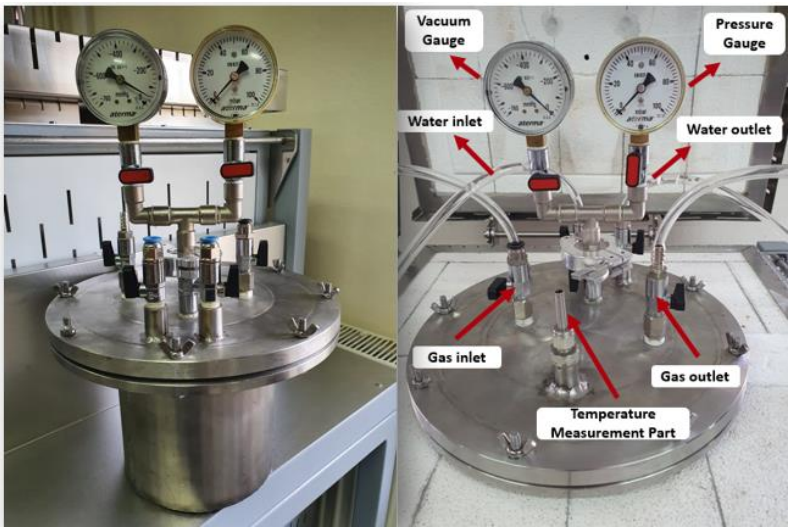

Figure 3.2. HDH reactor

The hydrogenation and dehydrogenation experiments were conducted in a steel reactor as seen in Figure which consists of vacuum and pressure gauges, water inlet and outlet for cooling the reactor lid, gas inlet and outlet, and a closed pipe for the temperature measurement. Onset time of the hydrogenation was observed by vacuum and pressure gauges with pressure changes. Water inlet and outlet parts were used to cool the gas released during the experiment and the exact internal temperature of the reactor was controlled by thermocouple.

Figure 3.3. High temperature resistance furnace

Figure shows high temperature resistance furnace (PROTHERM) where hydrogenation and dehydrogenation were carried out. As seen in Figure 3.2 and Figure 3.8, the design of the furnace offers easy placement of the reactor. The working temperature can be adjusted up to 1500°C.

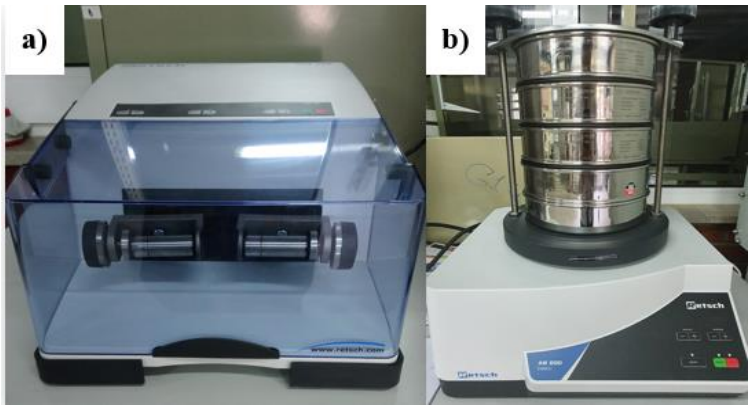

Figure 3.4. a) Ball mill b) Vibratory sieve shaker

Retsch MIXER MILL MM 200 (Figure3.4a) was used for the dry milling process. Milling is carried out by radial oscillations of the two grinding jars (10 mL) with maximum two stainless steel balls (Ø=7 mm) for each in a horizontal position up to 25 Hz that also causing in intense mixing of the sample. Retsch AS 200 BASIC (Figure 3.4b) was used to sieve and determine the particle size of hydrogenated powders. The sieving is carried out up to 100 Hz with driving electromagnetic for efficient separation.

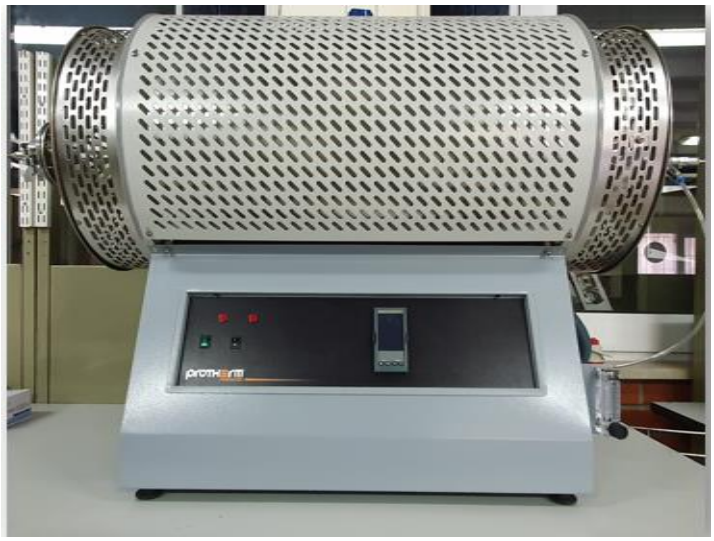

Figure 3.5. Tube Furnace

Tube furnace (PROTHERM), shown in Figure 3.5, was used in the hydrogenation and dehydrogenation processes. The working temperature can be set up to 1600°C. Gas and vacuum coupling halves on both ends of the tube control the gas inlet and outlet and samples are placed from there. O-ring which is placed between metal coupling halve parts keeps the vacuum of the setup.

Figure 3.6. Glove box

Glove box (INERT) was used in order to protect titanium powder from oxygen. Samples are placed enclosed area from transfer chambers seen in Figure 3.6 and the level of oxygen and moisture in the enclosed are less than 1 ppm.

Figure 3.7. Vacuum pump

Vacuum pump (Figure 3.7) was used to evacuate air from reactor for cleaning and provide vacuum atmosphere for the dehydrogenation experiments.

3.3 Methods

3.3.1 Size reduction Ti-6Al-2Sn-4Zr-6Mo turnings via ball milling

In order to determine the size reduction ability of the turnings without the hydrogenation, as-received Ti-6Al-2Sn-4Zr-6Mo turnings with the same thickness were milled at different frequencies and durations as tabulated in Table3.3.

Table 3.3. Parameters of milling process for as-received Ti-6Al-2Sn-4Zr-6Mo turnings

Trial number	Alloy	Thickness before milling (mm)	Frequency (Hz)	Duration (min)
1	Ti-6Al-2Sn-4Zr-6Mo	9.7	20	10
2	Ti-6Al-2Sn-4Zr-6Mo	9.7	25	20
3	Ti-6Al-2Sn-4Zr-6Mo	9.7	25	25

The maximum time for each milling step was set to 4 minutes to prevent the grinding jars from heating up and thus oxidation of titanium. A maximum of 1 gram of

turnings was used at each step to improve grinding quality and prevent ball abrasion that could cause contamination.

3.3.2 Cleaning of Ti-6Al-2Sn-4Zr-6Mo turnings

Turnings were cleaned ultrasonically (ISOLAB) with acetone and rinsed with deionized water to remove lubricants from the surface of turnings. Afterward, the turnings were dried under a vacuum atmosphere at 70 °C to avoid further oxidation.

3.3.3 Hydrogenation of Ti-6Al-2Sn-4Zr-6Mo turnings

Before starting the HDH experiments of Ti-6Al-2Sn-4Zr-6Mo turnings, Titanium sponge was used for validation of the experimental setup.

Ti-6Al-2Sn-4Zr-6Mo turnings and deoxidizing Mg chips were placed in different ceramic crucibles and the reactor was placed in the furnace (PROTHERM) after the lid was closed. The reactor was vacuumed to evacuate the air and filled with argon gas. This cleaning procedure was repeated three times before each trial. Afterward, hydrogen gas was filled into the reactor and the furnace was heated up to the target temperature.

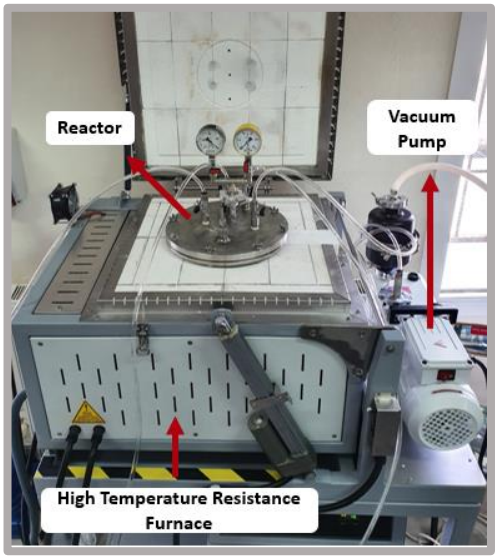

Figure 3.8. Schematic representation of the Hydrogenation- Dehydrogenation setup

Table 3.4. Parameters for the Hydrogenation experiments

Trial	Raw Material	Hydrogenation Temperature (°C)	Holding Time (min)	Type of gas flow	Heating rate (°C/min)	Deoxidizer
1	Titanium sponge	600	15	H_2		-
2	Ti-6246 turnings	600	15	H_2	5	Mg
3		600	15	H_2	5	-
4		600	15	H_2	20	Mg
5		400	60	H_2	5	Mg
6		500	60	H_2	5	Mg
7		600	60	H_2	5	Mg
8		500	120	H_2	5	Mg
9		500	120	Ar- H_2	5	-
10		600	120	Ar- H_2	5	-

The experimental set for the hydrogenation is tabulated in Table In order to reach the optimum the hydrogenation condition, some parameters including hydrogenation temperature and holding time, heating rate, usage of a deoxidizer, and hydrogen concentration were studied. Firstly, the effect of using a deoxidizer was investigated at 600°C for 15 minutes (trial 2 and 3). Then the heating rate was comparison was made in the trials 2 and 4. Hydrogenation was performed between 400-600 °C for one hour using deoxidizer (trials 2, 5, 6, 7) and holding time was increased to optimize both hydrogenation temperature and holding time in trial 8 to study the effect. Finally, the effect hydrogen concentration was investigated in trials 9 and 10. In addition, gas pressure and temperature changes were monitored with gauges during the process. An

increase in temperature and a decrease in pressure were expected since hydrogenation is an exothermic reaction.

3.3.4 Milling of hydrogenated Ti-6Al-2Sn-4Zr-6Mo turnings

Hydrogenated Ti-6Al-2Sn-4Zr-6Mo turnings were milled by using a ball mill (Retsch MIXER MILL MM 200) at 25 Hz with different durations. Turnings were placed in a grinding jar (10 mL) with stainless steel grinding balls (Ø=7 mm) to obtain hydride powder. After milling, the powders were sieved and classified according to the particle size for the next step (dehydrogenation). For sieving and classification of powders, test sieves (Haver & Boecker, Ø =200 mm) with different mesh sizes as 40,63 and 100 μm were selected. Vibratory sieve shaker (Retsch AS 200 BASIC) was used to achieve high separation efficiency with 80 Hz for 5 minutes.

3.3.5 Dehydrogenation of hydrogenated Ti-6Al-2Sn-4Zr-6Mo powders

The experimental set for the dehydrogenation is tabulated in Table Dehydrogenation experiments were carried out under a vacuum atmosphere with different temperatures and holding times to obtain titanium powders. A vacuum was used to evacuate the hydrogen gas released from the titanium matrix to avoid re-hydrogenation during cooling Hydride powders were placed in the reactor and the reactor was purged under Argon gas flow to remove oxygen from the environment. After the argon gas flow was stopped, the furnace was heated up to the target temperature under continuous vacuum.

Table 3.5. Parameters of the Dehydrogenation experiments

Trial	Raw Material	Dehydrogenation Temperature (°C)	Holding Time (min)
1	Ti-6246 hydride powder	600	90

(Cont. on next page)

Table 3.5. (cont.)

2	Ti-6246 hydride powder	620	120
3		650	120
4		650	120

The dehydrogenation temperatures were set higher than the related hydrogenation temperatures for all trials. Furthermore, the effect of particle size on dehydrogenation was examined. Also, temperature and gas pressure variation were observed as with the hydrogenation process. It was expected that the temperature would decrease and the pressure would increase in this endothermic process.

3.3.6 Characterization methods

The morphology of the turnings, hydrogenated turnings and powders and powders after dehydrogenation were determined by Scanning Electron Microscopy (SEM; FEI Quanta 250 FEG, USA). Size distribution of particles were estimated statistically from SEM micrographs using ImageJ software and using Mastersizer 2000. Hydrogen and oxygen concentration in powders were analyzed by hydrogen and oxygen analyzer (LECO ONH 836). The phase analyses of hydrogenated and dehydrogenated powder were carried out by X-ray Diffraction (XRD; PhilipsX'Pert Pro, Eindhoven, The Netherlands) with CuKα radiation (2Θ = 20°-80° and with scanning step as 0.005°/second).

CHAPTER 4

RESULTS & DISCUSSION

4.1 Size reduction behaviour of Ti-6Al-2Sn-4Zr-6Mo turnings during milling

The thickness of as-received Ti-6Al-2Sn-4Zr-6Mo turnings after milling with different frequencies and durations are tabulated in Table 4.1. As the frequency and duration increased, the thickness of turnings decreased but it was not desired level.

Table 4.1. Parameters of milling process for Ti-6Al-2Sn-4Zr-6Mo turnings before hydrogenation

Trial number	Alloy	Thickness before milling (mm)	Thickness after milling (mm)	Frequency (Hz)	Duration (min)
1	Ti-6Al-2Sn-4Zr-6Mo	9.7	4.6	20	10
2	Ti-6Al-2Sn-4Zr-6Mo	9.7	3.5	25	20
3	Ti-6Al-2Sn-4Zr-6Mo	9.7	2.3	25	25

As seen in Figure 4.1 powder could not be obtained even with the highest frequencies and duration as for 25 minutes with 25 Hz. It is well understood that a suitable process is needed to obtain powder from turnings.

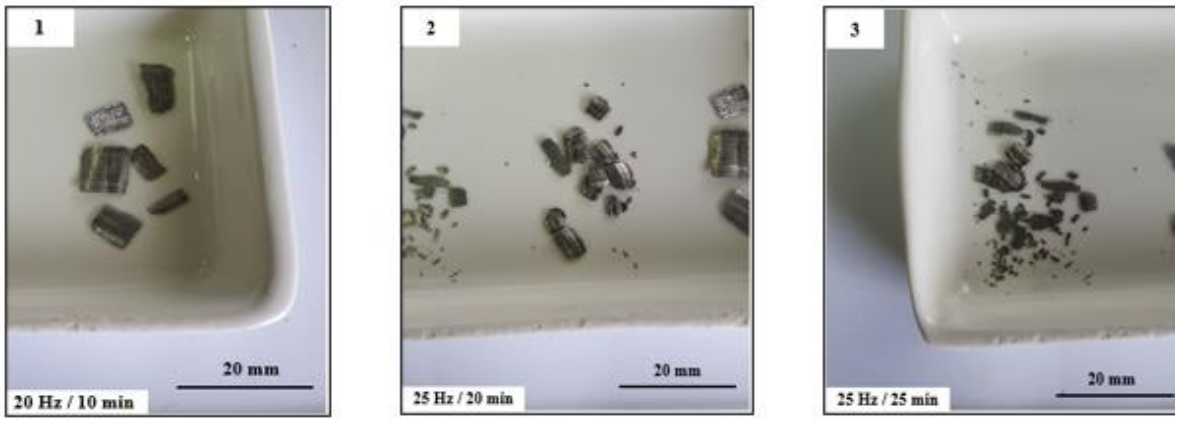

Figure 4.1. Effect of milling frequency and time on the size reduction of Ti- 6Al-2Sn-4Zr-6Mo turnings

4.2 Hydrogenation of Ti-6Al-2Sn-4Zr-6Mo turnings

Some qualitative results like colour change as seen in Figure 4.2 and embrittlement were obtained at the end of each hydrogenation experiment. Table introduces the hydrogenation parameters of titanium sponge and Ti-6Al-2Sn-4Zr-6Mo turning for each trial quantitative and qualitative results of hydrogenation experiments. Furthermore, hydrogen gas pressure started to decrease at 468 °C from which point hydrogen gas was continuously supplied to support hydrogenation of turnings in the HDH reactor. Temperature rise was not observed distinctively because small amount of turnings was used for hydrogenation.

Table 4.2. Quantitative and qualitative results of hydrogenation experiments

Trial	**A**	**B (°C)**	**C (min)**	**D**	**E (°C/min)**	**F**	**G**	**H**
1	Titanium sponge	600	15	H_2		-	+	+
2	Ti-6246 turnings	600	15	H_2	5	Mg	-	+
3		600	15	H_2	5	-	+	+

(Cont. on next page)

Table 4.2. (cont.)

4	Ti-6246 turnings	600	15	H_2	20	Mg	+	+
5		400	60	H_2	5	Mg	-	-
6		500	60	H_2	5	Mg	-	+
7		600	60	H_2	5	Mg	-	+
8		500	120	H_2	5	Mg	-	+
9		500	120	Ar-H_2	5	-	+	-
10		600	120	Ar-H_2	5	-	+	-

A:*Raw material* ***B:****Hydrogenation Temperature* ***C:****Holding Time* ***D:****Type of gas flow* ***E:****Heating rate* ***F:****Deoxidizer* ***G:****Colour Change* ***H:****Brittlement*

As mentioned before, increasing oxygen concentration in titanium leads to change in colour and formation different titanium oxides. The colour change follows this order; grey to yellow, yellow to purple and purple to blue so on as tabulated in Table 2.9.

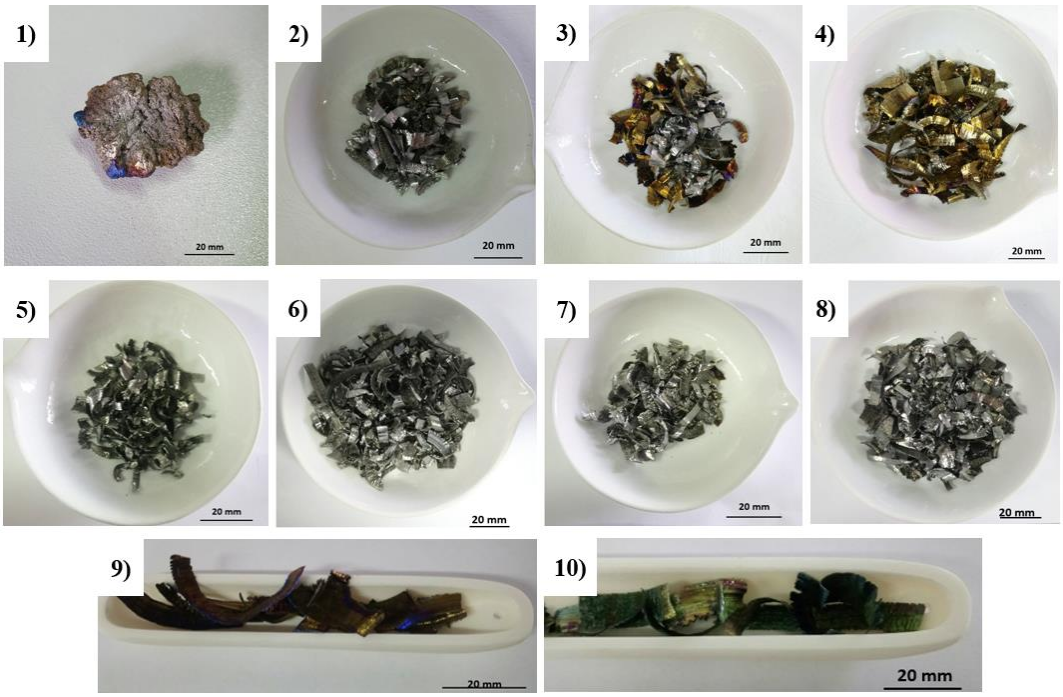

Figure 4.2. Colours after hydrogenation of Titanium sponge and Ti-6Al-2Sn-4Zr-6Mo turnings for trial 1-10

Hydrogenation of the Titanium sponge was performed to ensure the experimental setup at 600°C for 15 minutes. The titanium sponge was easily milled at the end of the hydrogenation. XRD pattern of hydrogenated Titanium sponge is given Figure 4.3. According to the XRD pattern of Titanium sponge, titanium hydride phases as $TiH_{1.924}$ were observed that supports the embrittlement. The same experimental parameters were also applied to Ti-6Al-2Sn-4Zr-6Mo turnings.

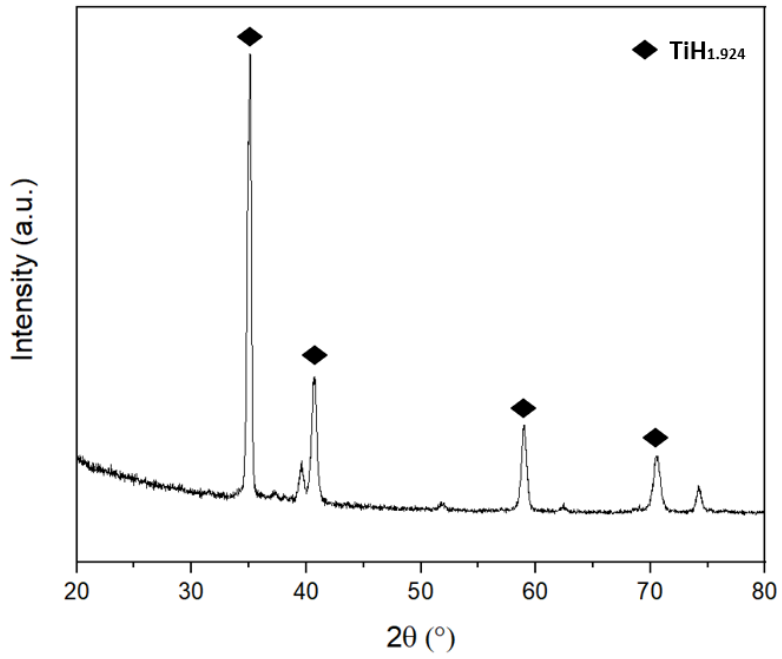

Figure 4.3. XRD pattern of hydrogenated Titanium sponge at 600° C for 15 minutes

Figure 4.4 presents precipitation of titanium hydride phases as $TiH_{1.924}$ with low density in titanium matrix. Moreover, the titanium phase was also detected which proves uncomplete hydrogenation. Furthermore, the colour change was not observed in the turnings after hydrogenation.

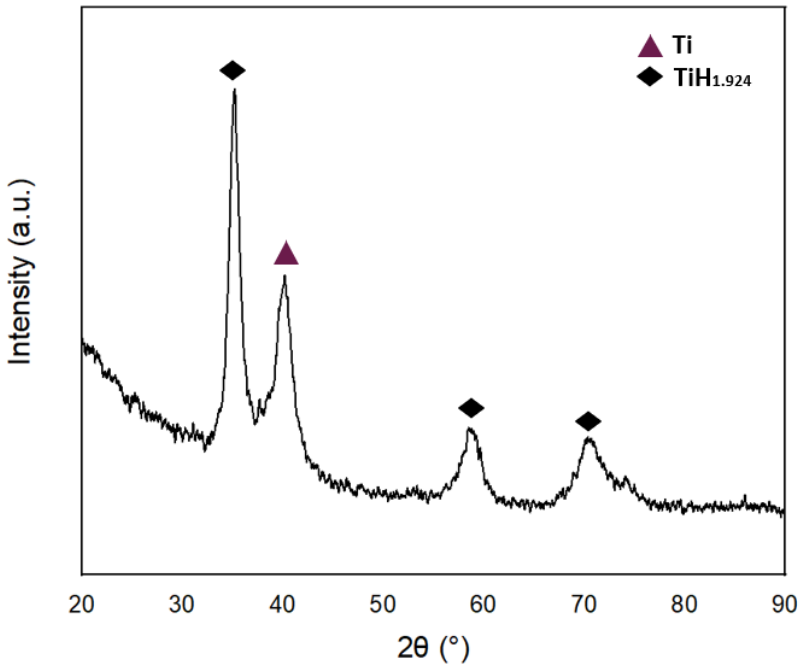

Figure 4.4. XRD pattern of hydrogenated Ti-6Al-2Sn-4Zr-6Mo turnings at 600° C for 15 minutes

4.2.1 Effect of using deoxidizer

The effect of the use of magnesium as the deoxidizer was examined and it was observed that the colour of some turnings turned yellow and purple when deoxidizer was not used as seen in Figure 4.2.3.

Figure 4.5 shows XRD pattern of turnings with different colours. While no hydride phase was observed in grey turnings, TiH1.924 phase was observed in yellow and purple ones. However, brittleness was achieved for all turnings. Moreover, titanium oxides were not detected in the pattern. It is known that colour change indicates oxidation and purple ones have higher oxygen concentrations. Also, titanium oxide acts as a stable surface oxide. Colour change may have occurred only on the surface, so it may not have much effect on the total concentration. That's why any oxide peaks were not observed in XRD pattern.

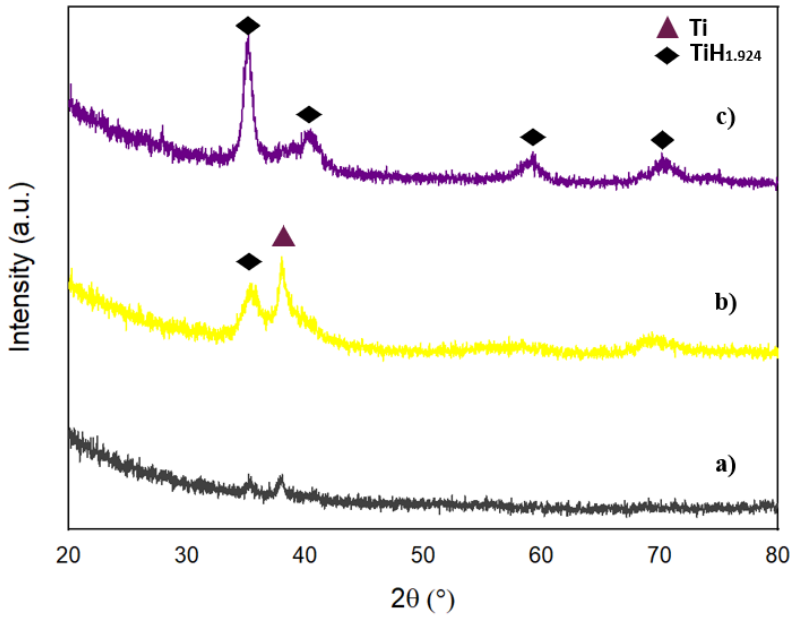

Figure 4.5. XRD pattern of hydrogenated a) grey b) yellow c) purple Ti-6Al-2Sn-4Zr-6Mo turnings at 600° C for 15 minutes without deoxidizer

- Colour change was observed on turnings when deoxidizer was not used. No correlation could be established regarding colour change, embrittlement and oxide formation.

4.2.2 Effect of heating rate on the hydrogenation of Ti-6Al-2Sn-4Zr-6Mo turnings

One of the parameters examined was the heating rate during the hydrogenation process. When the heating rate was increased from 5 to 20 °C/minute, almost all turnings turned yellow. Furthermore, the embrittlement of the turnings was not at desired level. The titanium hydride phase was not precipitated and titanium phase was observed alone in the XRD pattern as shown in Figure 4.6. This can arise from that the increased exposure time leading to the surface spalling and promoting the formation of a new surface on the material surface (Tal-Gutelmacher and Eliezer 2005). Accordingly, hydrogenation is easily accomplished as a new surface begins to form with longer exposure time.

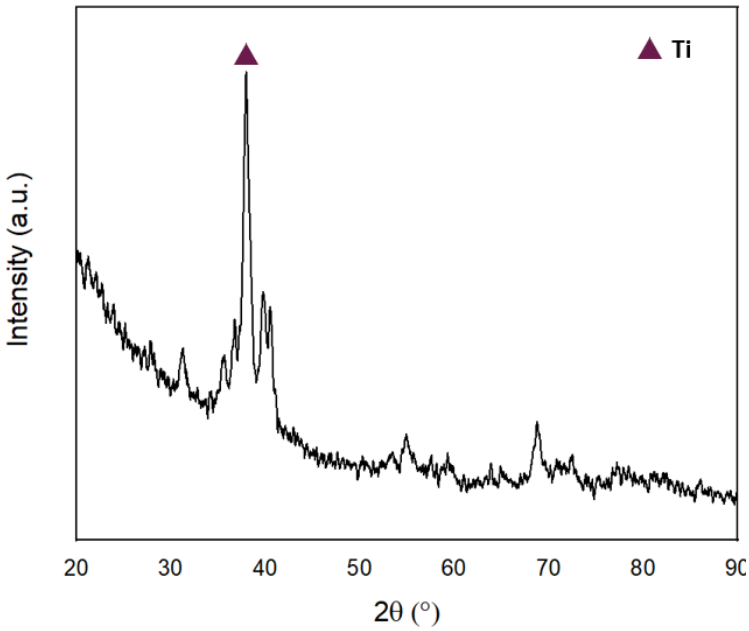

Figure 4.6. XRD pattern of hydrogenated Ti-6Al-2Sn-4Zr-6Mo turnings at 600° C for 15 minutes with 20 °C/minute heating rate

- As the exposure time increases, new surface formation on the turnings can be promoted and therefore the heating rate should be as low as possible. The heating rate was selected to a low rate as 5°C/minute for further the hydrogenation experiments.

4.2.3 Effect of temperature and holding time on the hydrogenation of Ti-6Al-2Sn-4Zr-6Mo turnings

The effect of increasing temperature on the formation of the titanium hydride phase is given in Figure 4.7. According to the XRD pattern, higher temperatures promote formation of hydride phases with high intensity. Moreover, sharper hydride peaks were obtained at 600 °C for 60 minutes.

The hydrogenation temperature was studied in the experimental set where the temperature was between 400-600 °C. Hydrogen embrittlement was not accomplished at 400°C, whereas Ti-6Al-2Sn-4Zr-6Mo turnings were easily crushed into powders at 500 °C and 600 °C for 60 minutes.

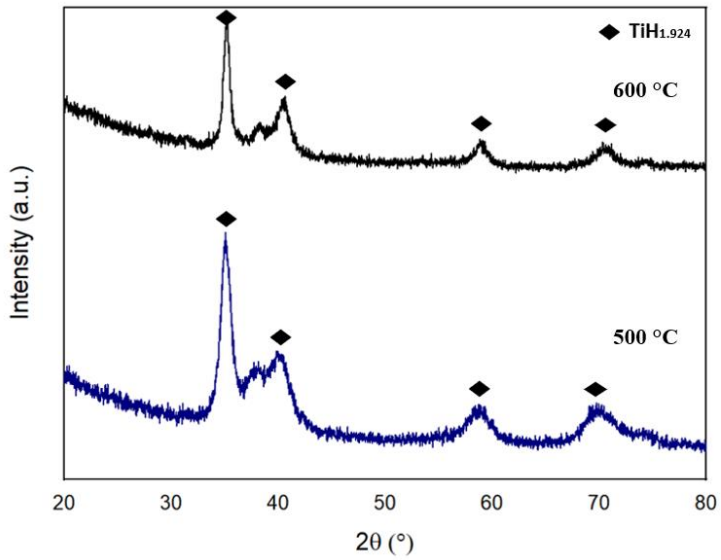

Figure 4.7. XRD patterns of hydrogenated Ti-6Al-2Sn-4Zr-6Mo turnings at different temperatures for 60 minutes

After the hydrogenation temperature was set to 500 °C, the effect of holding time on hydrogenation was investigated. Figure 4.8 demonstrates the amount of hydrogen in the hydride phase increases with increasing holding time. All peaks in the pattern are TiH_2 which prove reaching optimum condition for hydrogenation.

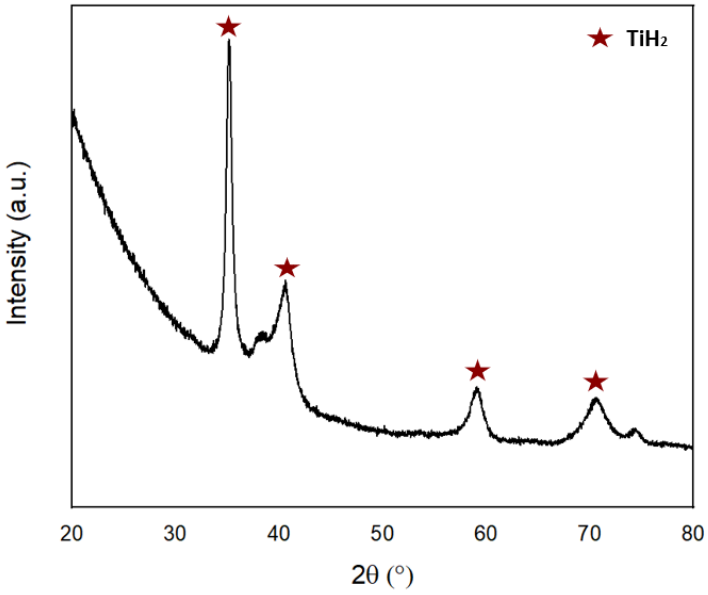

Figure 4.8. XRD pattern of hydrogenated Ti-6Al-2Sn-4Zr-6Mo turnings at 500 °C for 120 minutes

- Hydrogen embrittlement and hydride formation were promoted by increasing temperature and holding time as 500 °C for 120 minutes.

4.2.4 Particle size analysis of Ti-6Al-2Sn-4Zr-6Mo hydride and HDH powder

Figure 4.9 presents the particle size distribution of hydrogenated Ti-6Al-2Sn-4Zr-6Mo powders at 500 °C for 120 minutes. According to result, size of hydride powders lies between 1.096 – 181.970 μm and mean particle size is around 56 μm. It is well understood that hydrogenation was carried out successfully at 500 °C for two hours because of its capability of production finer powder.

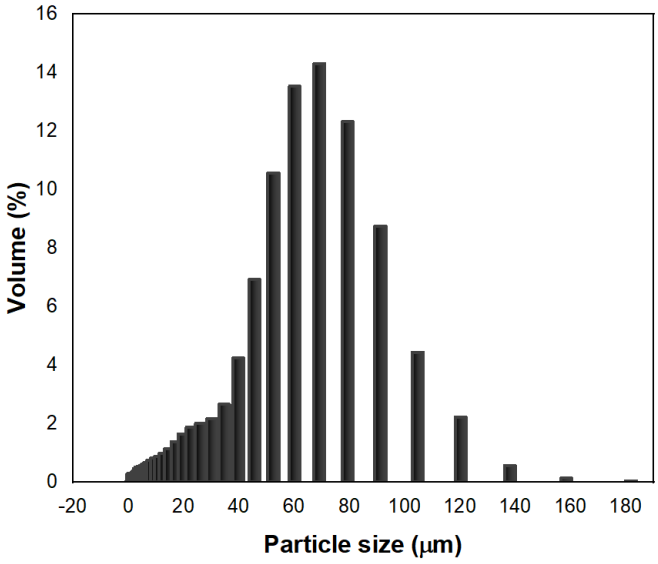

Figure 4.9. Particle size analysis for hydrogenated Ti-6Al-2Sn-4Zr-6Mo powders at 500 °C for 120 minutes

The particle size distribution was also reported by using ImageJ software for each particle separately both longest and shortest axes because of its non-spherical shape. Since this analysis is done manually, it gives rough estimate when compared to the particle size analyser. As presented in Figure 4.10 the mean of particle size distribution shifts to smaller size as from 46 μm to 25 μm for smallest axis and from 87 μm to 28 μm for longest axis with the increasing hydrogenation temperature and holding time.

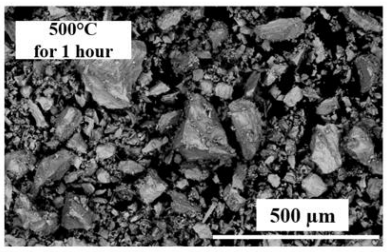

a)

for minimum axis

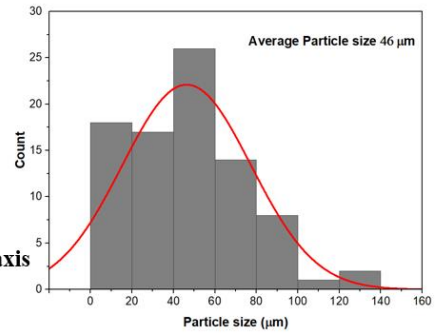

b)

for maximum axis

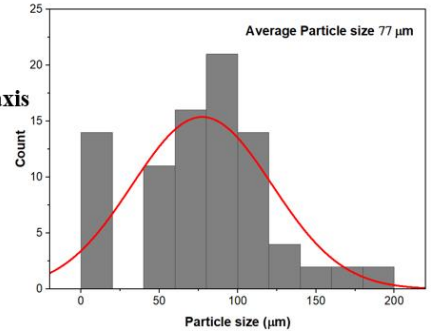

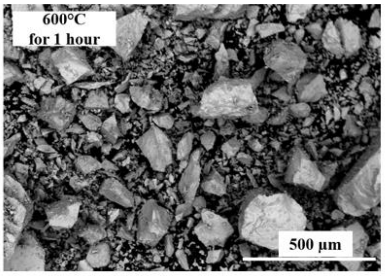

c)

for minimum axis

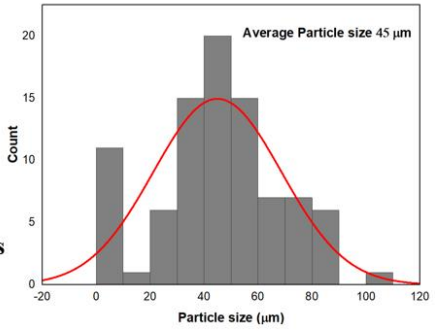

d)

for maximum axis

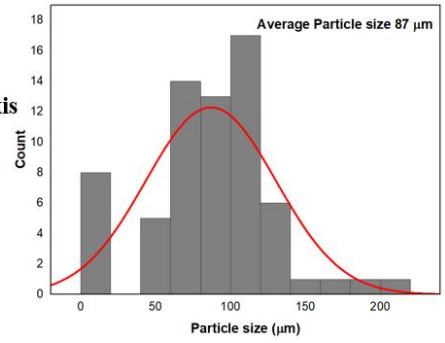

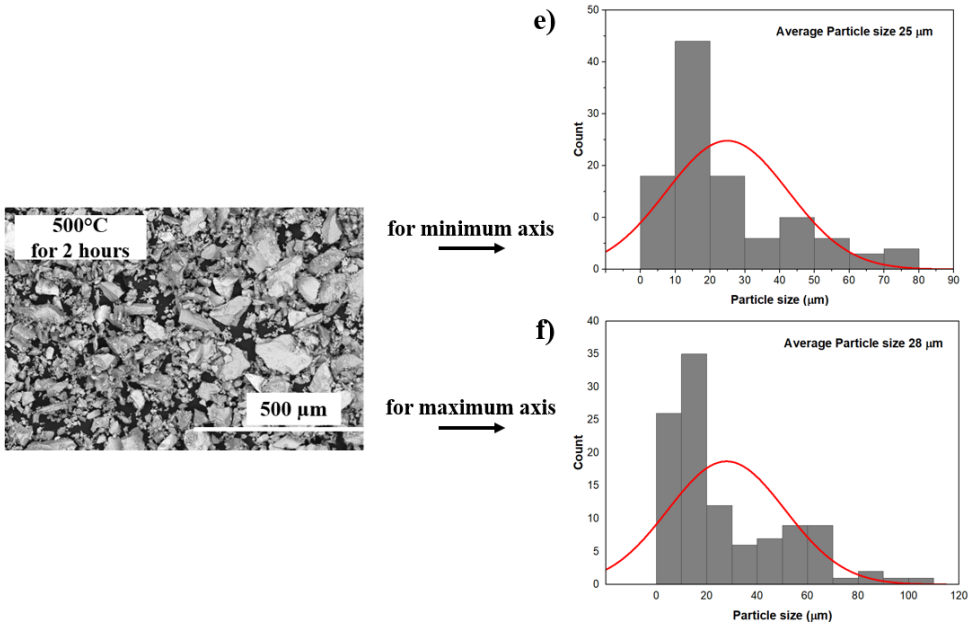

Figure 4.10. (a-f) SEM micrograph and particle size distribution hydrogenated Ti-6Al-2Sn-4Zr-6Mo powders at different temperatures and holding times

Furthermore, sieve analysis was performed and hydrogenated Ti-6Al-2Sn-4Zr-6Mo powders were classified as <40 µm, 40-63 µm, 63-100 µm and >100 µm after milling at 25 Hz for 15 minutes and mass distributions were recorded for each trial. Figure 4.11 demonstrates finer particles are obtained with higher amount by increasing hydrogenation temperature and holding time.

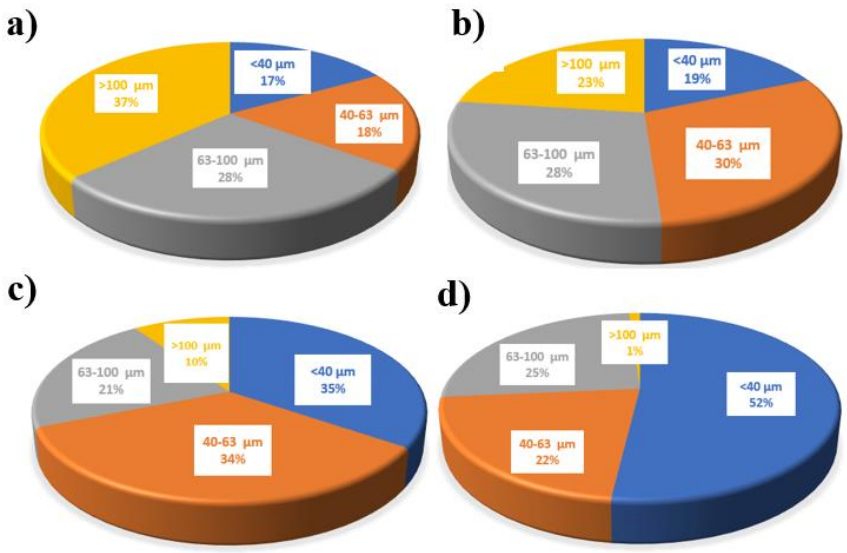

Figure 4.11. Mass distribution after sieving of hydrogenated Ti-6Al-2Sn-4Zr-6Mo powders at a) 600°C for 15 minutes b) 500°C for 60 minutes c) 600°C for 60 minutes d) 500°C for 120 minutes

- It was concluded that the hydrogenation temperature and holding time should be set as 500°C for 120 minutes to complete hydrogenation of Ti-6Al-2Sn-4Zr-6Mo and obtain easily finer hydride powders with an average particle size of 56 μm.

4.2.5 The morphology of hydrogenated Ti-6Al-2Sn-4Zr-6Mo turnings and powders and HDH powders

Figure 4.12 presents fractured surface of hydrogenated Ti-6246 turnings at 500 °C and 600 °C. These micrographs confirm that increasing hydrogen concentration on the Titanium matrix leads to brittle facets on surface and enhances crack propagation and embrittlement as also presented in Figure 4.12c reference micrograph (Tal-Gutelmacher and Eliezer 2005).

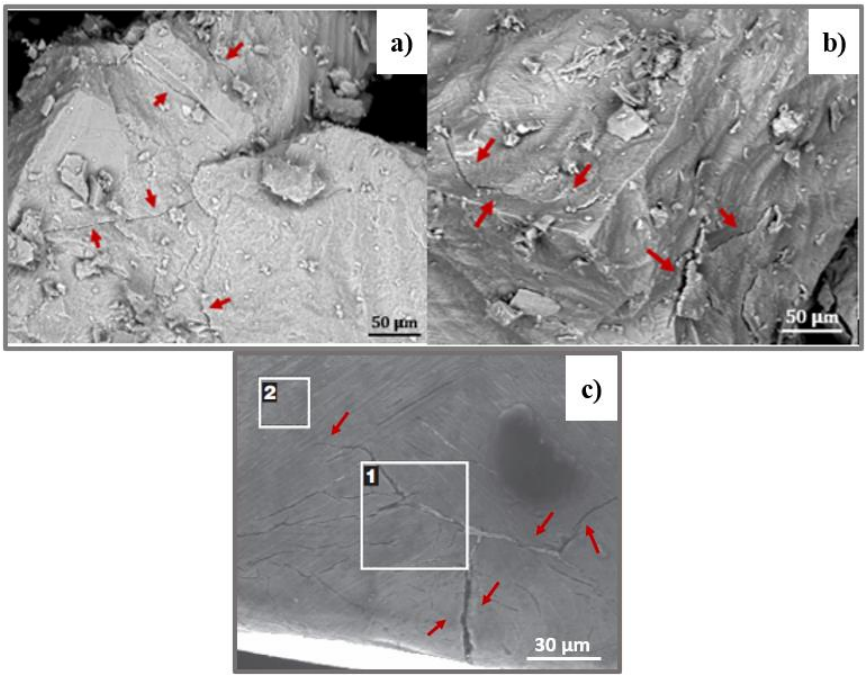

Figure 4.12. SEM images of hydrogenated Ti-6Al-2Sn-4Zr-6Mo turnings at a) 500 °C and b) 600 °C for 60 minutes c) reference micrograph

The morphology of hydrogenated Ti-6Al-2Sn-4Zr-6Mo powders at 500 °C and 600 °C for 60 minutes and 500 °C for 120 minutes is given in Figure 4.13. SEM images show non-spherical shaped powders were obtained after the hydrogenation process. It

has been documented in previous works that powders obtained after hydrogenation is not spherical because of the milling effect (Kim et al. 2014).

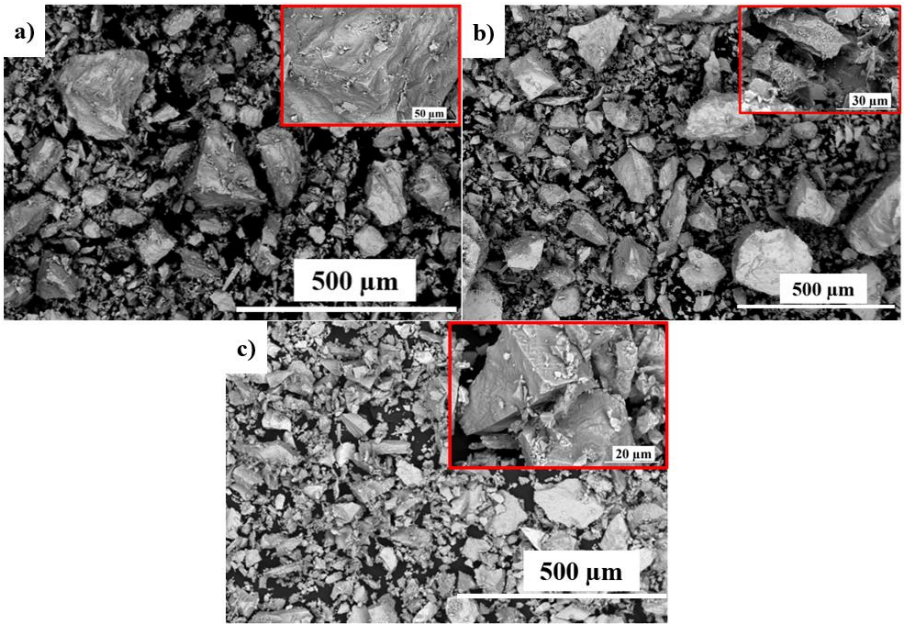

Figure 4.13. SEM images of hydrogenated Ti-6Al-2Sn-4Zr-6Mo powders at a) 500 °C for 60 minutes b) 600 °C for 60 minutes c) 500 °C for 120 minutes

SEM image of the HDH powder is presented in Figure 4.14a. As seen in micrograph, morphology of HDH powder is non-spherical which is also confirmed by calculation of aspect ratio distribution as demonstrated in Figure 4.14b. Mean aspect ratio was found 0.69. It is documented that aspect ratio for spherical particles should be 1. Also, there was no agglomeration after dehydrogenation process, so milling was not carried out again.

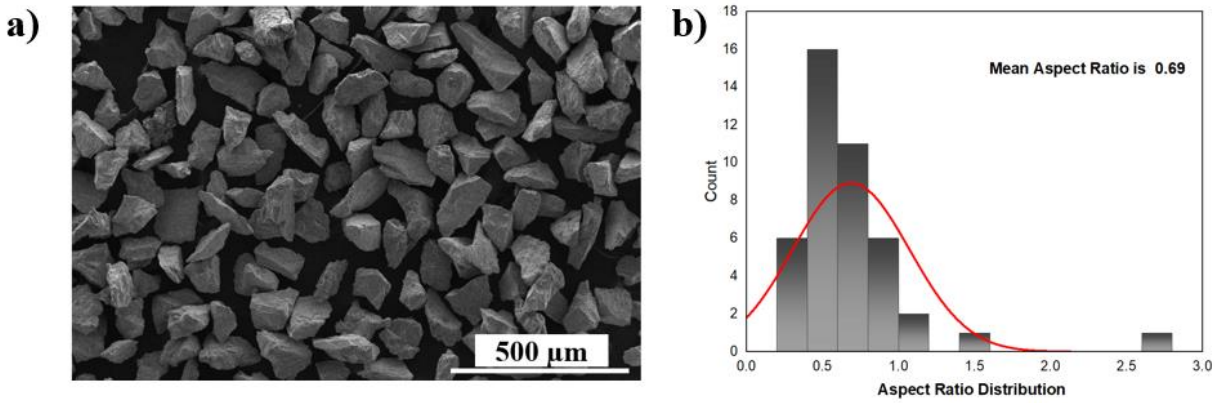

Figure 4.14. a) SEM image of HDH powder b) Mean aspect ratio of HDH powder

- From size and morphology point of view, HDH powders can be used in many applications like metal injection moulding, hot isostatic pressing and selective laser melting in terms of particle size. However, suitable process is needed to obtain spherical powder because of flowability that is limitation for use in additive manufacturing. Since non-spherical powders exhibit low flowability.

4.2.6 Effect of the hydrogen concentration on the hydrogenation of Ti-6Al-2Sn-4Zr-6Mo turnings

Ar-H_2 (95 % Ar + 5% H2) was used instead of high purity (99.999 %) H2 to examine effect of hydrogen concentration during the hydrogenation. Hydrogen embrittlement was not accomplished at both 500 °C and 600 °C for two hours. As seen in Figure 4.2.9-10 the turning colour changed from purple to light green with increasing temperature. Argon gas has higher density than hydrogen gas and Argon concentration is higher amount in this mixture. That's why hydrogen diffusion may be inhibited. High purity hydrogen atmosphere must be provided to achieve hydrogenation.

- In conclusion, high purity hydrogen environment should be provided during hydrogenation to achieve hydrogen embrittlement.

Figure 4.15 shows free energy of the formation of TiH_2 and TiO_2 versus different temperatures. At 500 °C free energy of the formation of TiH_2 is around -9.26 kJ/mol while free energy of formation of TiO_2 is -191.91 kJ/mol at the same temperature. According to diagram, formation of TiO_2 is more favourable than formation of TiH_2 at all temperatures. It is well understood that hydrogenation was carried out successfully instead of oxidation in our hydrogenation experiments.

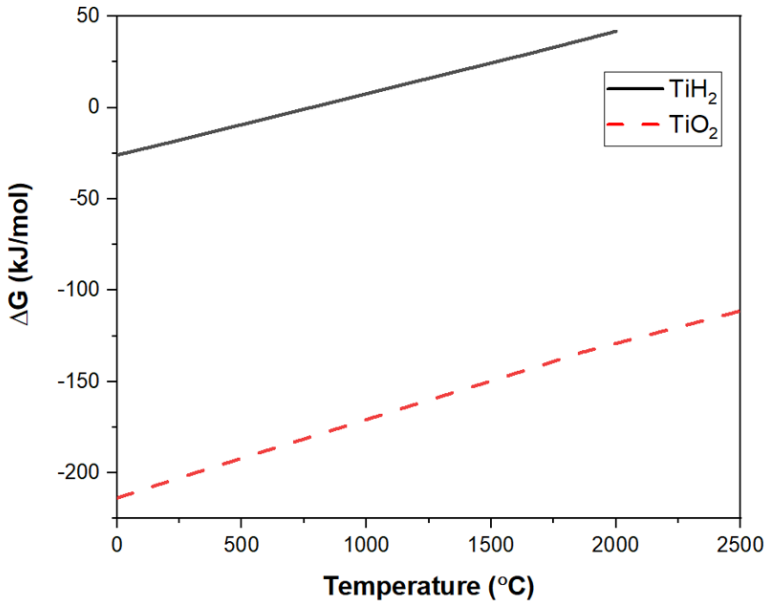

Figure 4.15. Free energy of the formation of TiH_2 and TiO_2

Figure 4.16 shows TGA results at 800 °C with 5 °C/minutes heating rate at argon flow. To investigate the dehydrogenation temperatures and effect of particle size on dehydrogenation temperatures, TGA analysis was carried out. Mass loss was observed in only 40-63 µm powders and it started first at 183.2 °C. Until 183.2 °C, 0.6% mass gain was observed and the 0.6% mass gain is completely reduced at 506.3 °C. After this point, an increase in mass was always detected. Mass gain can arise from oxidation of titanium powders. Both <40 and 63-100 µm powders exhibit only mass gain with different velocities. While rate of mass gain reduced at 596 °C for <40 µm powders, it was observed for 63-100 µm powders at 593.2 °C. Hydrogen can be removed at these temperatures. That's why dehydrogenation temperatures were set as around 600 °C for both <40 and 63-100 µm powders

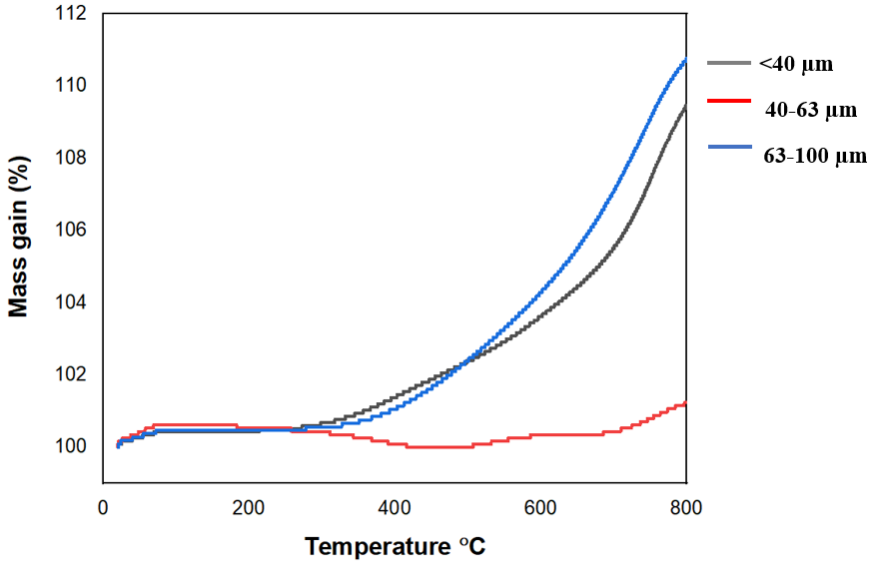

Figure 4.16. TGA analysis of the hydrogenated Ti-6Al-2Sn-4Zr-6Mo powders according to the particle size <40 ,40-63 and 63-100 µm

4.3 Dehydrogenation of hydrogenated Ti-6Al-2Sn-4Zr-6Mo powders

From a thermodynamical point of view, the hydrogenation reaction is an exothermic reaction where ΔH<0 and

$$\Delta G = \Delta H - T\Delta S \quad (13)$$

formation of titanium hydride takes place spontaneously where ΔG<0. It is also known that metal hydride formation is a reversible reaction, that's why dehydrogenation temperatures were set higher than hydrogenation temperatures to obtain titanium powder. In order to examine the effect of particle size on dehydrogenation, hydride powders were classified according to particle size as <40, 40-63 and 63-100 µm and dehydrogenation experiments were carried out at suitable temperatures

Table 4.3. Mass gain (%) after the dehydrogenation according to particle size

					Mass gain (%)		
Trial	**Hyd. T. (°C)**	**Holding Time (min)**	**Dehyd. T. (°C)**	**Holding Time (min)**	**<40 µm**	**40-63 µm**	**63-100 µm**
1	500	120	600	90	not classified		
2	600	15	620	120	34.45	13.93	4.24
3	500	60	650	120	19.41	15.48	7.03
4	600	60	650	120	32.06	14.70	3.54

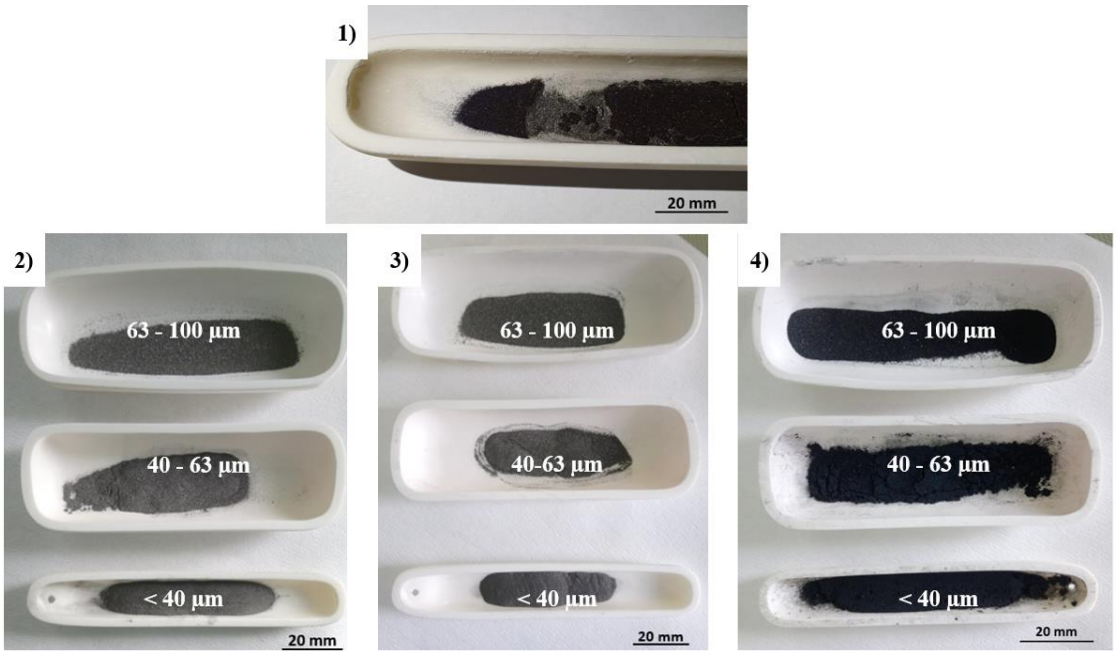

Figure 4.17. Colours after dehydrogenation of Ti-6Al-2Sn-4Zr-6Mo hydride powder for trial 1-4 (powers are classified for 2,3 and 4 trials)

Mass gain (%) after the dehydrogenation according to particle size is tabulated in Table 4.3. It is well understood that finer particles <40 µm have the largest surface area and are prone to oxidation and thus the mass increase was greatest for finer particles. Also, hydrogen gas pressure began to increase and the vacuum value began to decrease at 604 °C. Since a small amount of turnings was also used for the dehydrogenation, no obvious temperature decrease was observed.

Figure 4.18 shows XRD pattern of the dehydrogenated Ti-6Al-2Sn-4Zr-6Mo hydride powder at 600 °C for 90 minutes. Two different coloured layers grey and purple were obtained after dehydrogenation and classified as their colour for analysis as shown in Figure 4.17.1. It is seen in the XRD pattern that Titanium hydride phases were not observed and all hydride peaks changed as titanium in both powders which proves complete dehydrogenation. Also, any oxide phase was not detected in titanium matrix. That's why we can also conclude that vacuum atmosphere was provided at desired level that prevents oxidation although high oxygen affinity of titanium at elevated temperatures.

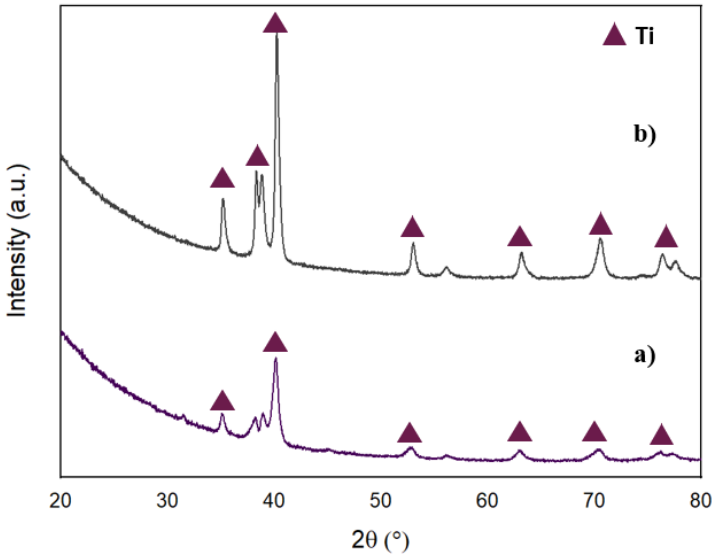

Figure 4.18. XRD pattern of the HDH powders dehydrogenated at 600 °C for 90 minutes for a) purple powder b) grey powder

Hydrogenated Ti-6Al-2Sn-4Zr-6Mo powder was classified as <40 ,40-63 and 63-100 µm prior to dehydrogenation trials to examine effect of particle size on dehydrogenation in subsequent experiments.

As seen in Figure 4.19, dehydrogenation was accomplished for both powders with <40 and 40-63 µm particles whereas the titanium hydride peak as TiH 1.924 was observed in 63-100 µm particles. Moreover, Ti3O and TiO2 phases were precipitated in a titanium matrix. According to Table 4.4, finer particles have higher oxygen concentrations as 26.3667 % while they have a lower hydrogen concentration as 0.068 %.

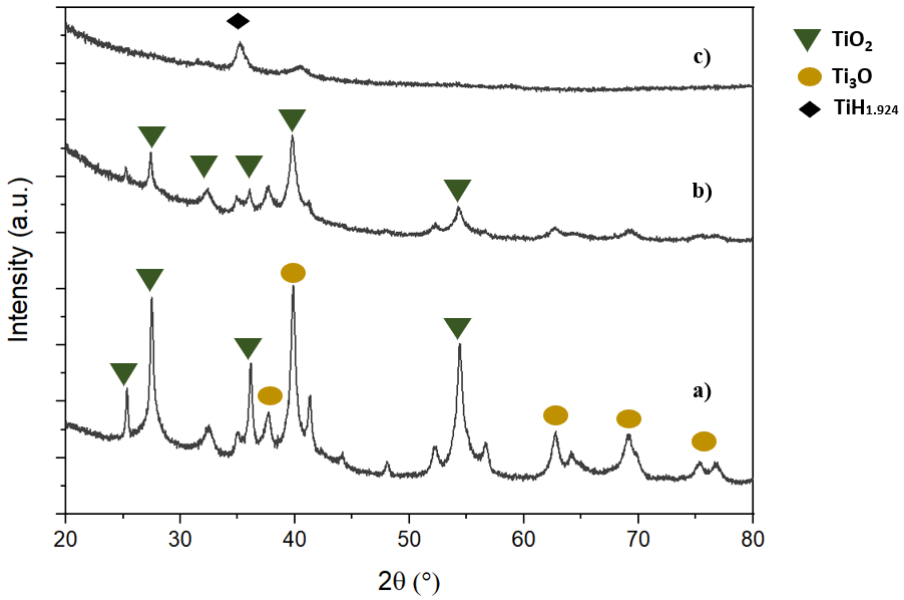

Figure 4.19. XRD pattern of HDH powders dehydrogenated at 620 °C for 120 minutes with different particle sizes a) <40 µm b) 40-63 µm c) 63-100 µm

Table 4.4. Elemental analysis of the dehydrogenated Ti-6Al-2Sn-4Zr-6Mo hydride at 620 °C for 120 minutes

Particle Size	Oxygen (%)	Hydrogen (%)	Nitrogen (%)
<40 µm	26.3667	0.0683	34.4667
63-100 µm	4.5033	0.4373	0.2850

XRD pattern of the dehydrogenation of Ti-6Al-2Sn-4Zr-6Mo hydride powder at 650 °C for 120 minutes is given in Figure 4.20. It is seen that dehydrogenation was accomplished for all powders. Furthermore, hydrogen and oxygen concentration were decreased with increasing temperature from 620 to 650 °C as tabulated in Table 4.5.

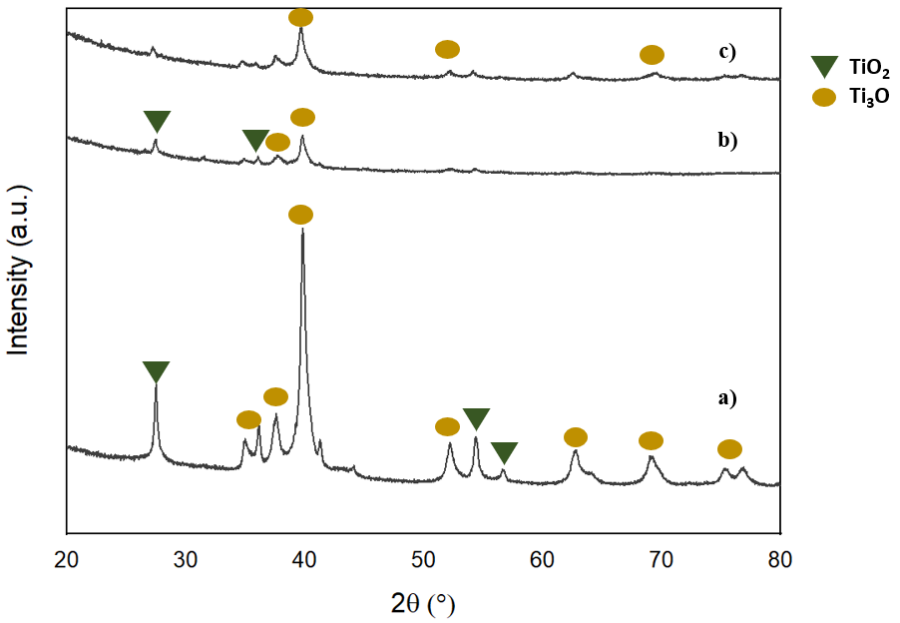

Figure 4.20. XRD pattern of HDH powders dehydrogenated at 650 °C for 120 minutes with different particle sizes a) <40 µm b) 40-63 µm and c) 63-100 µm

Table 4.5. Elemental analysis of the dehydrogenated Ti-6Al-2Sn-4Zr-6Mo hydride at 650 °C for 120 minutes

Particle Size	Oxygen (%)	Hydrogen (%)	Nitrogen (%)
<40 µm	17.7333	0.0487	0.3077
63-100 µm	8.7933	0.3263	0.0555

Figure 4.21 presents XRD pattern of dehydrogenation of another Ti-6Al-2Sn-4Zr-6Mo powder at 650 °C for 120 minutes. It is seen that dehydrogenation was accomplished for both powders with <40 and 40-60 µm particles whereas the titanium hydride peaks as $TiH_{1.924}$ were observed in 63-100 µm particles. It is also confirmed by hydrogen content analysis as seen in Table 4.6 while hydrogen concentration is 0.0665 % for <40 µm powder, this value is 0.518% for 63-100 µm powder.

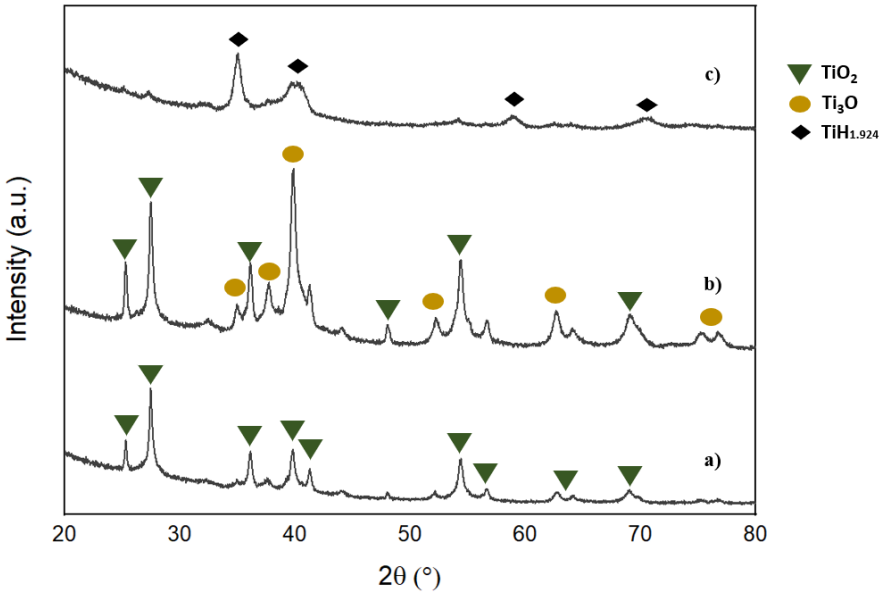

Figure 4.21. XRD pattern of the HDH powders dehydrogenated at 650 °C for 120 minutes with different particle sizes a) <40 µm b) 40-63 µm and c) 63-100 µm

Table 4.6. Elemental analysis of the dehydrogenated Ti-6Al-2Sn-4Zr-6Mo hydride at 650 °C for 120 minutes

Particle Size	Oxygen (%)	Hydrogen (%)	Nitrogen (%)
<40 µm	26.0333	0.0665	4.2772
63-100 µm	5.89	0.518	0.1980

The high amount of oxygen may be caused by the lack of an inert environment during milling and the ineffective use of the glove box. The amount of oxygen can be reduced with a suitable process like deoxygenation.

- To sum up briefly to the dehydrogenation results, dehydrogenation was achieved generally for <40 µm powder with highest oxygen content. This can arise from finer particles tend to oxidize more easily, so oxidation is more favourable when sufficient vacuum cannot be provided. That's why high oxidation capability can promote the dehydrogenation in finer powders at insufficient vacuum atmosphere.

CHAPTER 5

CONCLUSION

In this thesis, HDH was used as the experimental method which is a promising option in comparison to other titanium powder metallurgy methods. Ti-6Al-2Sn-4Zr-6Mo turning was used as raw material to examine the capacity of the HDH process to synthesize titanium powder from secondary sources.

- Hydrogenation of Ti-6Al-2Sn-4Zr-6Mo turnings was started at 468 °C where hydrogen pressure began to decrease.
- Dehydrogenation of hydride powders was observed at 604 °C with increasing hydrogen gas pressure.
- Hydrogenation experiment was optimized at 500 °C for 120 minutes with 5 °C/minute heating rate.
- Increasing the hydrogenation temperature and holding time promoted to obtain higher amount fine Ti-6Al-2Sn-4Zr-6Mo hydride powder with average 56 μm particle size.
- The powders obtained after the HDH process were non-spherical (aspect ratio 0.69) that suitable process is needed in order not to restrict their use in various fields like additive manufacturing where spherical powder are preferred.

CHAPTER 6

FUTURE PROSPECTIVES

- High amount of O_2 and H_2 content in the HDH powders will reduce by a suitable process like deoxygenation, supplying inert atmosphere during milling and vacuum atmosphere during both hydrogenation and dehydrogenation processes and effective use of glove box.
- The usability of synthesized powders will be examined.

REFERENCES

Alam, M. K., S. L. Semiatin, and Z. Ali. 1998. “Thermal Stress Development during Vacuum Arc Remelting and Permanent Mold Casting of Ingots.” *Journal of Manufacturing Science and Engineering, Transactions of the ASME* 120 (4): 755–63. https://doi.org/10.1115/1.2830216.

Bania, Paul J. 1994. “Beta Titanium Alloys and Their Role in the Titanium Industry.” *JOM* 46 (7): 16–19. https://doi.org/10.1007/BF03220742.

Barbis, Daniel P., Robert M. Gasior, Graham P. Walker, Joseph A. Capone, and Teddi S. Schaeffer. 2015. “Titanium Powders from the Hydride-Dehydride Process.” In *Titanium Powder Metallurgy: Science, Technology and Applications*, 101–16. Elsevier Inc. https://doi.org/10.1016/B978-0-12-800054-0.00007-1.

Bolzoni, L., E. M. Ruiz-Navas, and E. Gordo. 2012. “Influence of Vacuum Hot-Pressing Temperature on the Microstructure and Mechanical Properties of Ti-3Al-2.5V Alloy Obtained by Blended Elemental and Master Alloy Addition Powders.” *Materials Chemistry and Physics* 137 (2): 608–16. https://doi.org/10.1016/j.matchemphys.2012.10.010.

Boyer, R. R. 1996. “An Overview on the Use of Titanium in the Aerospace Industry.” *Materials Science and Engineering A* 213 (1–2): 103–14. https://doi.org/10.1016/0921-5093(96)10233-1.

Caiazzo, Fabrizia, Vittorio Alfieri, Gaetano Corrado, Paolo Argenio, Giuseppe Barbieri, Francesco Acerra, and Vincenzo Innaro. 2017. “Laser Beam Welding of a Ti–6Al–4V Support Flange for Buy-to-Fly Reduction.” *Metals* 7 (5). https://doi.org/10.3390/met7050183.

Centeno-Sánchez, R. Lilia, Derek J. Fray, and George Z. Chen. 2007. “Study on the Reduction of Highly Porous TiO2 Precursors and Thin TiO2 Layers by the FFC-Cambridge Process.” *Journal of Materials Science* 42 (17): 7494–7501. https://doi.org/10.1007/s10853-007-1588-8.

Che-Haron, C. H. 2001. “Tool Life and Surface Integrity in Turning Titanium Alloy.” In *Journal of Materials Processing Technology*, 118:231–37. https://doi.org/10.1016/S0924-0136(01)00926-8.

Chen, Lian, Yong He, Yingxin Yang, Shiwei Niu, and Haitao Ren. 2017. “The Research Status and Development Trend of Additive Manufacturing Technology.” *International Journal of Advanced Manufacturing Technology*. Springer London. https://doi.org/10.1007/s00170-016-9335-4.

Chen, W., Y. Yamamoto, W. H. Peter, S. B. Gorti, A. S. Sabau, M. B. Clark, S. D. Nunn, et al. 2011. “Cold Compaction Study of Armstrong Process® Ti-6Al-4V Powders.” *Powder Technology* 214 (2): 194–99. https://doi.org/10.1016/j.powtec.2011.08.007.

Cotton, James D., Robert D. Briggs, Rodney R. Boyer, Sesh Tamirisakandala, Patrick Russo, Nikolay Shchetnikov, and John C. Fanning. 2015. “State of the Art in Beta Titanium Alloys for Airframe Applications.” *JOM*. Minerals, Metals and Materials Society. https://doi.org/10.1007/s11837-015-1442-4.

Crowley, Grant. 2003. “How to Extract Low-Cost Titanium.” *Advanced Materials and Processes* 161 (11): 25–27.

Dunstan, Matthew K., Avi Gordon, James D. Paramore, and Brady G. Butler. 2019. “Feasibility of Using Titanium Machine Turnings in Powder Metallurgy Processes.” *JOM* 71 (5): 1831–39. https://doi.org/10.1007/s11837-019-03400-3.

Entezarian, M., F. Allaire, P. Tsantrizos, and R. A.L. Drew. 1996. “Plasma Atomization: A New Process for the Production of Fine, Spherical Powders.” *JOM* 48 (6): 53–55. https://doi.org/10.1007/BF03222969.

Ezugwu, E. O., and Z. M. Wang. 1997. “Titanium Alloys and Their Machinability - A Review.” *Journal of Materials Processing Technology* 68 (3): 262–74. https://doi.org/10.1016/S0924-0136(96)00030-1.

Faller, Kurt, and F. H. Froes. 2001. “The Use of Titanium in Family Automobiles: Current Trends.” *JOM* 53 (4): 27–28. https://doi.org/10.1007/s11837-001-0143-3.

Fang, Zhigang Zak, James D. Paramore, Pei Sun, K. S.Ravi Chandran, Ying Zhang, Yang Xia, Fei Cao, Mark Koopman, and Michael Free. 2018. “Powder Metallurgy

of Titanium–Past, Present, and Future." *International Materials Reviews* 63 (7): 407–59. https://doi.org/10.1080/09506608.2017.1366003.

Festas, António, António Ramos, and João Paulo Davim. 2022. "Machining of Titanium Alloys for Medical Application - a Review." *Proceedings of the Institution of Mechanical Engineers, Part B: Journal of Engineering Manufacture*. SAGE Publications Ltd. https://doi.org/10.1177/09544054211028531.

Florkiewicz, Wioletta, Dagmara Malina, Bożena Tyliszczak, and Agnieszka Sobczak-Kupiec. 2020. "Manufacturing of Titanium and Its Alloys." In *Studies in Systems, Decision and Control*, 198:61–74. Springer International Publishing. https://doi.org/10.1007/978-3-030-11274-5_5.

Fray, Derek. 2016. "Molten Salts and Energy Related Materials." *Faraday Discussions* 190: 11–34. https://doi.org/10.1039/c6fd00090h.

Froes, F. H., H. Friedrich, J. Kiese, and D. Bergoint. 2004. "Titanium in the Family Automobile: The Cost Challenge." *JOM*. Minerals, Metals and Materials Society. https://doi.org/10.1007/s11837-004-0144-0.

Fujita, Takahiro, Atsushi Ogawa, Chiaki Ouchi, and Hidenori Tajima. 1996. "Microstructure and Properties of Titanium Alloy Produced in the Newly Developed Blended Elemental Powder Metallurgy Process." *Materials Science and Engineering A* 213 (1–2): 148–53. https://doi.org/10.1016/0921-5093(96)10232-X.

Gao, Yanfeng, Gui Wang, and Binbin Liu. 2016. "Chip Formation Characteristics in the Machining of Titanium Alloys: A Review." *International Journal of Machining and Machinability of Materials* 18 (1–2): 155–84. https://doi.org/10.1504/IJMMM.2016.075467.

Gemelli, E., and N.H.A. Camargo. 2007. "Oxidation Kinetics of Commercially Pure Titanium." *Matéria (Rio de Janeiro)* 12 (3): 525–31. https://doi.org/10.1590/s1517-70762007000300014.

Gerling, R., H. Clemens, and F. P. Schimansky. 2004. "Powder Metallurgical Processing of Intermetallic Gamma Titanium Aluminides." *Advanced Engineering Materials*. Wiley-VCH Verlag. https://doi.org/10.1002/adem.200310559.

Gurrappa, I. 2003. “Characterization of Titanium Alloy Ti-6Al-4V for Chemical, Marine and Industrial Applications.” *Materials Characterization* 51 (2–3): 131–39. https://doi.org/10.1016/j.matchar.2003.10.006.

Hamweendo, Agripa, Terence Malama, and Ionel Botef. 2016. “Titanium-Nickel Alloys for Bone Tissue Engineering Application via Cold Spray.” *International Conference on Competitive Manufacturing*, no. JANUARY. https://doi.org/10.13140/RG.2.1.4046.9527.

Hassanin, Hany, Yahya Zweiri, Laurane Finet, Khamis Essa, Chunlei Qiu, and Moataz Attallah. 2021. “Laser Powder Bed Fusion of Ti-6al-2sn-4zr-6mo Alloy and Properties Prediction Using Deep Learning Approaches.” *Materials* 14 (8). https://doi.org/10.3390/ma14082056.

Hu, Di, Aleksei Dolganov, Mingchan Ma, Biyash Bhattacharya, Matthew T. Bishop, and George Z. Chen. 2018. “Development of the Fray-Farthing-Chen Cambridge Process: Towards the Sustainable Production of Titanium and Its Alloys.” *JOM* 70 (2): 129–37. https://doi.org/10.1007/s11837-017-2664-4.

Imam, M. Ashraf, and F. H. Froes. 2010. “Low Cost Titanium and Developing Applications.” *JOM* 62 (5): 17–20. https://doi.org/10.1007/s11837-010-0069-8.

Jang, Tae Sik, Dong Eung Kim, Ginam Han, Chang Bun Yoon, and Hyun do Jung. 2020. “Powder Based Additive Manufacturing for Biomedical Application of Titanium and Its Alloys: A Review.” *Biomedical Engineering Letters*. Springer Verlag. https://doi.org/10.1007/s13534-020-00177-2.

Joshi, Vydehi Arun. 2006. *Titanium Alloys: An Atlas of Structures and Fracture Features*. *Materials Characterization*. CRC Press.

Kim, Youngmoo, Eun Pyo Kim, Young Beom Song, Sung Ho Lee, and Young Sam Kwon. 2014. “Microstructure and Mechanical Properties of Hot Isostatically Pressed Ti-6Al-4V Alloy.” *Journal of Alloys and Compounds* 603 (August): 207–12. https://doi.org/10.1016/j.jallcom.2014.03.022.

Kroll, W. 1940. “The Production of Ductile Titanium.” *Transactions of The Electrochemical Society* 78 (1): 35. https://doi.org/10.1149/1.3071290.

Larminie, James, and Andrew Dicks. 2003. *Fuel Cell Systems Explained*. *Fuel Cell Systems Explained*. John Wiley & Sons, Ltd,. https://doi.org/10.1002/9781118878330.

Luo, Liangshun, Yanqing Su, Jingjie Guo, and Hengzhi Fu. 2006. "Formation of Titanium Hydride in Ti-6Al-4V Alloy." *Journal of Alloys and Compounds* 425 (1–2): 140–44. https://doi.org/10.1016/j.jallcom.2006.01.014.

Lutjering, G, and J C Williams. 2007. *Titanium - 2nd Edition*. Edited by Brian Derby. *Engineering Materials and Processes*. Springer-Verlag.

Ma, Meng, Dihua Wang, Wenguang Wang, Xiaohong Hu, Xianbo Jin, and George Z. Chen. 2006. "Extraction of Titanium from Different Titania Precursors by the FFC Cambridge Process." *Journal of Alloys and Compounds* 420 (1–2): 37–45. https://doi.org/10.1016/j.jallcom.2005.10.048.

Mitkov, M., and D. Božić. 1996. "Hydride-Dehydride Conversion of Solid Ti6Al4V to Powder Form." *Materials Characterization* 37 (2–3): 53–60. https://doi.org/10.1016/s1044-5803(96)00061-7.

Moll, John H. 2000. "Utilization of Gas-Atomized Titanium and Titanium-Aluminide Powder." *JOM* 52 (5): 32–34. https://doi.org/10.1007/s11837-000-0030-3.

Nachtrab, W.T., P.R. Roberts, and H.A. Newborn. 1992. "Powder Metallurgy of Advanced Titanium Alloys." *Key Engineering Materials* 77–78 (January): 115–40. https://doi.org/10.4028/www.scientific.net/kem.77-78.115.

Nagesh, Ch R.V.S., C. S. Ramachandran, and R. B. Subramanyam. 2008. "Methods of Titanium Sponge Production." *Transactions of the Indian Institute of Metals* 61 (5): 341–48. https://doi.org/10.1007/s12666-008-0065-7.

Numakura, H., M. Koiwa, H. Asano, H. Murata, and F. Izumi. 1986. "X-Ray Diffraction Study on the Formation of γ Titanium Hydride." *Scripta Metallurgica* 20 (2): 213–16. https://doi.org/10.1016/0036-9748(86)90128-6.

Oh, Jung Min, Ki Min Roh, Back Kyu Lee, Chang Youl Suh, Wonbaek Kim, Hanjung Kwon, and Jae Won Lim. 2014. "Preparation of Low Oxygen Content Alloy Powder from Ti Binary Alloy Scrap by Hydrogenation-Dehydrogenation and

Deoxidation Process." *Journal of Alloys and Compounds* 593 (April): 61–66. https://doi.org/10.1016/j.jallcom.2014.01.033.

Pan, Long, Chun Ming Wang, Su Fen Xiao, and Yun Gui Chen. 2019. "Hydrogenation Behaviors and Characteristics of Bulk Ti–6Al–4V Alloy at Different Isothermal Temperatures." *Rare Metals* 38 (12): 1131–35. https://doi.org/10.1007/s12598-016-0852-y.

Peters, Manfred, Jörg Kumpfert, Charles H. Ward, and Christoph Leyens. 2003. "Titanium Alloys for Aerospace Applications." *Advanced Engineering Materials*. https://doi.org/10.1002/adem.200310095.

Peters, Manfred, and Christopher Leyens. 2003. *Titanium and Titanium Alloys: Fundamentals and Applications*. *Titanium and Titanium Alloys Fundamentals and Applications*. Vol. 1. Wiley.

Prasad, Soni, Mark Ehrensberger, Monica Prasad Gibson, Hyeongil Kim, and Edward A. Monaco. 2015. "Biomaterial Properties of Titanium in Dentistry." *Journal of Oral Biosciences*. Japanese Association for Oral Biology. https://doi.org/10.1016/j.job.2015.08.001.

Qian, M., and D. L. Bourell. 2017. "Additive Manufacturing of Titanium Alloys." *JOM*. Minerals, Metals and Materials Society. https://doi.org/10.1007/s11837-017-2630-1.

Roberts, P. R. 1989. "Production of PREP Titanium Powder." In *1989 Advances in Powder Metallurgy - Volume 3*, 427–38. Publ by MPIF Metal Powder Industries Federation.

Sam Froes, Francis H. 2015. "A Historical Perspective of Titanium Powder Metallurgy." In *Titanium Powder Metallurgy: Science, Technology and Applications*, 1–19. Elsevier Inc. https://doi.org/10.1016/B978-0-12-800054-0.00001-0.

San-Martin, A., and F. D. Manchester. 1987. "The H-Ti (Hydrogen-Titanium) System." *Bulletin of Alloy Phase Diagrams* 8 (1): 30–42. https://doi.org/10.1007/BF02868888.

Schwandt, Carsten. 2013. “Understanding the Electro-Deoxidation of Titanium Dioxide to Titanium Metal via the FFC-Cambridge Process.” In *Transactions of the Institutions of Mining and Metallurgy, Section C: Mineral Processing and Extractive Metallurgy*, 122:213–18. https://doi.org/10.1179/0371955313Z.00000000071.

Schwandt, Carsten, Greg R. Doughty, and Derek J. Fray. 2010. “The FFC-Cambridge Process for Titanium Metal Winning.” In *Key Engineering Materials*, 436:13–25. Trans Tech Publications Ltd. https://doi.org/10.4028/www.scientific.net/KEM.436.13.

Sherman, A. M., and J. E. Allison. 1986. “Potential for Automotive Applications of Titanium Alloys.” In *SAE Technical Papers*. SAE International. https://doi.org/10.4271/860608.

Simona Baltatu, Madalina, Catalin Andrei Tugui, Manuela Cristina Perju, Marcelin Benchea, Mihaela Claudia Spataru, Andrei Victor Sandu, and Petrica Vizureanu. 2019. “Biocompatible Titanium Alloys Used in Medical Applications.” *Revista de Chimie* 70 (4): 1302–6. https://doi.org/10.37358/rc.19.4.7114.

Sohn, Ho-Sang. 2021. “Current Status of Titanium Recycling Technology.” *Resources Recycling* 30 (1): 26–34. https://doi.org/10.7844/kirr.2021.30.1.26.

Song, Yulai, Zhihe Dou, Ting an Zhang, and Yan Liu. 2020. “Research Progress on the Extractive Metallurgy of Titanium and Its Alloys.” *Mineral Processing and Extractive Metallurgy Review*. Taylor and Francis Inc. https://doi.org/10.1080/08827508.2020.1793145.

Spitans, Sergejs, Henrik Franz, and Egbert Baake. 2020. “Numerical Modeling and Optimization of Electrode Induction Melting for Inert Gas Atomization (EIGA).” *Metallurgical and Materials Transactions B: Process Metallurgy and Materials Processing Science* 51 (5): 1918–27. https://doi.org/10.1007/s11663-020-01934-5.

Sun, Pei, Zhigang Zak Fang, Ying Zhang, and Yang Xia. 2017. “Review of the Methods for Production of Spherical Ti and Ti Alloy Powder.” *JOM*. Minerals, Metals and Materials Society. https://doi.org/10.1007/s11837-017-2513-5.

Sun, Zhonggang, Hongliang Hou, Wenlong Zhou, Yaoqi Wang, and Zhiqiang Li. 2009. "The Effect of Hydrogen on Microstructures Evolution and Deformation Behaviors of Ti-6Al-4V Alloys." *Journal of Alloys and Compounds* 476 (1–2): 550–55. https://doi.org/10.1016/j.jallcom.2008.09.054.

Takeda, Osamu, Takanari Ouchi, and Toru H. Okabe. 2020. "Recent Progress in Titanium Extraction and Recycling." *Metallurgical and Materials Transactions B: Process Metallurgy and Materials Processing Science* 51 (4): 1315–28. https://doi.org/10.1007/s11663-020-01898-6.

Tal-Gutelmacher, Ervin, and Dan Eliezer. 2004. "Hydrogen-Assisted Degradation of Titanium Based Alloys." *Materials Transactions* 45 (5): 1594–1600. https://doi.org/10.2320/matertrans.45.1594.

Tal-Gutelmacher, Ervin, and Dan Eliezer. 2005. "The Hydrogen Embrittlement of Titanium-Based Alloys." *JOM*. Minerals, Metals and Materials Society. https://doi.org/10.1007/s11837-005-0115-0.

Thermodynamics - Interaction Studies - Solids, Liquids and Gases. 2012. *Thermodynamics - Interaction Studies - Solids, Liquids and Gases*. InTech. https://doi.org/10.5772/823.

Titanium Alloys - Novel Aspects of Their Manufacturing and Processing [Working Title]. 2019. *Titanium Alloys - Novel Aspects of Their Manufacturing and Processing [Working Title]*. IntechOpen. https://doi.org/10.5772/intechopen.78626.

Truong, Van Doi, Yong Taek Hyun, Jong Woo Won, Wonjoo Lee, and Jonghun Yoon. 2022. "Numerical Simulation of the Effects of Scanning Strategies on the Aluminum Evaporation of Titanium Alloy in the Electron Beam Cold Hearth Melting Process." *Materials* 15 (3). https://doi.org/10.3390/ma15030820.

Tsutsui, Tadayuki. 2012. "Recent Technology of Powder Metallurgy and Applications." *Hitachi Chemical Technical Report No.54*, no. 54: 12–20. http://www.hitachi-chem.co.jp/english/report/054/54_sou2.pdf.

Umeda, Junko, Takanori Mimoto, Hisashi Imai, and Katsuyoshi Kondoh. 2017. "Powder Forming Process from Machined Titanium Chips via Heat Treatment in

Hydrogen Atmosphere." *Materials Transactions* 58 (12): 1702–7. https://doi.org/10.2320/matertrans.Y-M2017833.

Veiga, C., J. P. Davim, and A. J.R. Loureiro. 2012. "Properties and Applications of Titanium Alloys: A Brief Review." *Reviews on Advanced Materials Science*.

Viteri, Virginia Senz de, and Elena Fuentes. 2013. "Titanium and Titanium Alloys as Biomaterials." In *Tribology - Fundamentals and Advancements*. InTech. https://doi.org/10.5772/55860.

Wang, Chunming, Yeguang Zhang, Yuhang Wei, Libo Mei, Sufen Xiao, and Yungui Chen. 2016. "XPS Study of the Deoxidization Behavior of Hydrogen in TiH2 Powders." *Powder Technology* 302 (November): 423–25. https://doi.org/10.1016/j.powtec.2016.09.005.

Wang, Dihua, Xianbo Jin, and George Z. Chen. 2008. "Solid State Reactions: An Electrochemical Approach in Molten Salts." *Annual Reports on the Progress of Chemistry - Section C* 104: 189–234. https://doi.org/10.1039/b703904m.

Wasz, M. L., F. R. Brotzen, R. B. McLellan, and A. J. Griffin. 1996. "Effect of Oxygen and Hydrogen on Mechanical Properties of Commercial Purity Titanium." *International Materials Reviews* 41 (1): 1–12. https://doi.org/10.1179/imr.1996.41.1.1.

Weiss, I., and S. L. Semiatin. 1998. "Thermomechanical Processing of Beta Titanium Alloys - An Overview." *Materials Science and Engineering A* 243 (1–2): 46–65. https://doi.org/10.1016/S0921-5093(97)00783-1.

Weiss, I., and S. L. Semiatin. 1999. "Thermomechanical Processing of Alpha Titanium Alloys - An Overview." *Materials Science and Engineering A*. Elsevier BV. https://doi.org/10.1016/s0921-5093(98)01155-1.

Williams, James C., and Rodney R. Boyer. 2020. "Opportunities and Issues in the Application of Titanium Alloys for Aerospace Components." *Metals* 10 (6). https://doi.org/10.3390/met10060705.

Woodside, C. Rigel, Paul E. King, and Chris Nordlund. 2013. "Arc Distribution during the Vacuum Arc Remelting of Ti-6Al-4V." *Metallurgical and Materials*

Transactions B: Process Metallurgy and Materials Processing Science 44 (1): 154–65. https://doi.org/10.1007/s11663-012-9760-1.

Wu, Tair I., and Jiann Kuo Wu. 2002. “Effects of Electrolytic Hydrogenating Parameters on Structure and Composition of Surface Hydrides of CP-Ti and Ti-6Al-4V Alloy.” *Materials Chemistry and Physics* 74 (1): 5–12. https://doi.org/10.1016/S0254-0584(01)00403-5.

Xia, Yang, Jinlong Zhao, Qinghua Tian, and Xueyi Guo. 2019. “Review of the Effect of Oxygen on Titanium and Deoxygenation Technologies for Recycling of Titanium Metal.” *JOM* 71 (9): 3209–20. https://doi.org/10.1007/s11837-019-03649-8.

Züttel, Andreas. 2003. “Materials for Hydrogen Storage.” *Materials Today* 6 (9): 24–33. https://doi.org/10.1016/S1369-7021(03)00922-2.